



OPEN ACCESS

EDITED BY

Daniel Nývlt,
Masaryk University, Czechia

REVIEWED BY

Matěj Roman,
Aberystwyth University, United Kingdom
Rienk H. Smittenberg,
Stockholm University, Sweden

*CORRESPONDENCE

Ulrike Herzschuh,
✉ ulrike.herzschuh@awi.de

RECEIVED 12 December 2023

ACCEPTED 02 April 2024

PUBLISHED 26 April 2024

CITATION

Baisheva I, Biskaborn BK,
Stoof-Leichsenring KR, Andreev A, Heim B,
Meucci S, Ushnitskaya LA, Zakharov ES,
Dietze E, Glückler R, Pstryakova LA and
Herzschuh U (2024), Late Glacial and
Holocene vegetation and lake changes in SW
Yakutia, Siberia, inferred from *sedaDNA*,
pollen, and XRF data.
Front. Earth Sci. 12:1354284.
doi: 10.3389/feart.2024.1354284

COPYRIGHT

© 2024 Baisheva, Biskaborn,
Stoof-Leichsenring, Andreev, Heim, Meucci,
Ushnitskaya, Zakharov, Dietze, Glückler,
Pstryakova and Herzschuh. This is an
open-access article distributed under the
terms of the [Creative Commons Attribution
License \(CC BY\)](https://creativecommons.org/licenses/by/4.0/). The use, distribution or
reproduction in other forums is permitted,
provided the original author(s) and the
copyright owner(s) are credited and that the
original publication in this journal is cited, in
accordance with accepted academic practice.
No use, distribution or reproduction is
permitted which does not comply with
these terms.

Late Glacial and Holocene vegetation and lake changes in SW Yakutia, Siberia, inferred from *sedaDNA*, pollen, and XRF data

Izabella Baisheva^{1,2,3}, Boris K. Biskaborn¹,
Kathleen R. Stoof-Leichsenring¹, Andrei Andreev¹, Birgit Heim¹,
Stefano Meucci^{1,4}, Lena A. Ushnitskaya³, Evgenii S. Zakharov³,
Elisabeth Dietze^{1,5}, Ramesh Glückler^{1,2}, Luidmila A. Pstryakova³
and Ulrike Herzschuh^{1,2,4*}

¹Polar Terrestrial Environmental Systems, Alfred Wegener Institute Helmholtz Centre for Polar and Marine Research, Potsdam, Germany, ²Institute for Environmental Science and Geography, University of Potsdam, Potsdam, Germany, ³Institute of Natural Sciences, North-Eastern Federal University of Yakutsk, Yakutsk, Russia, ⁴Institute for Biochemistry and Biology, University of Potsdam, Potsdam, Germany, ⁵Institute of Geography, Georg-August-University Göttingen, Göttingen, Lower Saxony, Germany

Only a few palaeo-records extend beyond the Holocene in Yakutia, eastern Siberia, since most of the lakes in the region are of Holocene thermokarst origin. Thus, we have a poor understanding of the long-term interactions between terrestrial and aquatic ecosystems and their response to climate change. The Lake Khamra region in southwestern Yakutia is of particular interest because it is in the transition zones from discontinuous to sporadic permafrost and from summergreen to evergreen boreal forests. Our multiproxy study of Lake Khamra sediments reaching back to the Last Glacial Maximum 21 cal ka BP, includes analyses of organic carbon, nitrogen, XRF-derived elements, sedimentary ancient DNA amplicon sequencing of aquatic and terrestrial plants and diatoms, as well as classical counting of pollen and non-pollen palynomorphs (NPP). The palaeogenetic approach revealed 45 diatom, 191 terrestrial plant, and 65 aquatic macrophyte taxa. Pollen analyses identified 34 pollen taxa and 28 NPP taxa. The inferred terrestrial ecosystem of the Last Glacial comprises tundra vegetation dominated by forbs and grasses, likely inhabited by megaherbivores. By 18.4 cal ka BP a lake had developed with a high abundance of macrophytes and dominant fragilarioid diatoms, while shrubs expanded around the lake. In the Bølling-Allerød at 14.7 cal ka BP both the terrestrial and aquatic systems reflect climate amelioration, alongside lake water-level rise and woodland establishment, which was curbed by the Younger Dryas cooling. In the Early Holocene warmer and wetter climate led to taiga development and lake water-level rise, reflected by diatom composition turnover from only epiphytic to planktonic diatoms. In the Mid-Holocene the lake water level decreased at ca. 8.2 cal ka BP and increased again at ca. 6.5 cal ka BP. At the same time mixed evergreen-summergreen forest expanded. In the Late Holocene, at ca. 4 cal ka BP, vegetation cover similar to modern conditions established. This study reveals

the long-term shifts in aquatic and terrestrial ecosystems and a comprehensive understanding of lake development and catchment history of the Lake Khamra region.

KEYWORDS

lake sediment, diatoms, macrophytes, non-pollen palynomorphs, palaeoreconstruction, tundra, boreal forest, refugia

1 Introduction

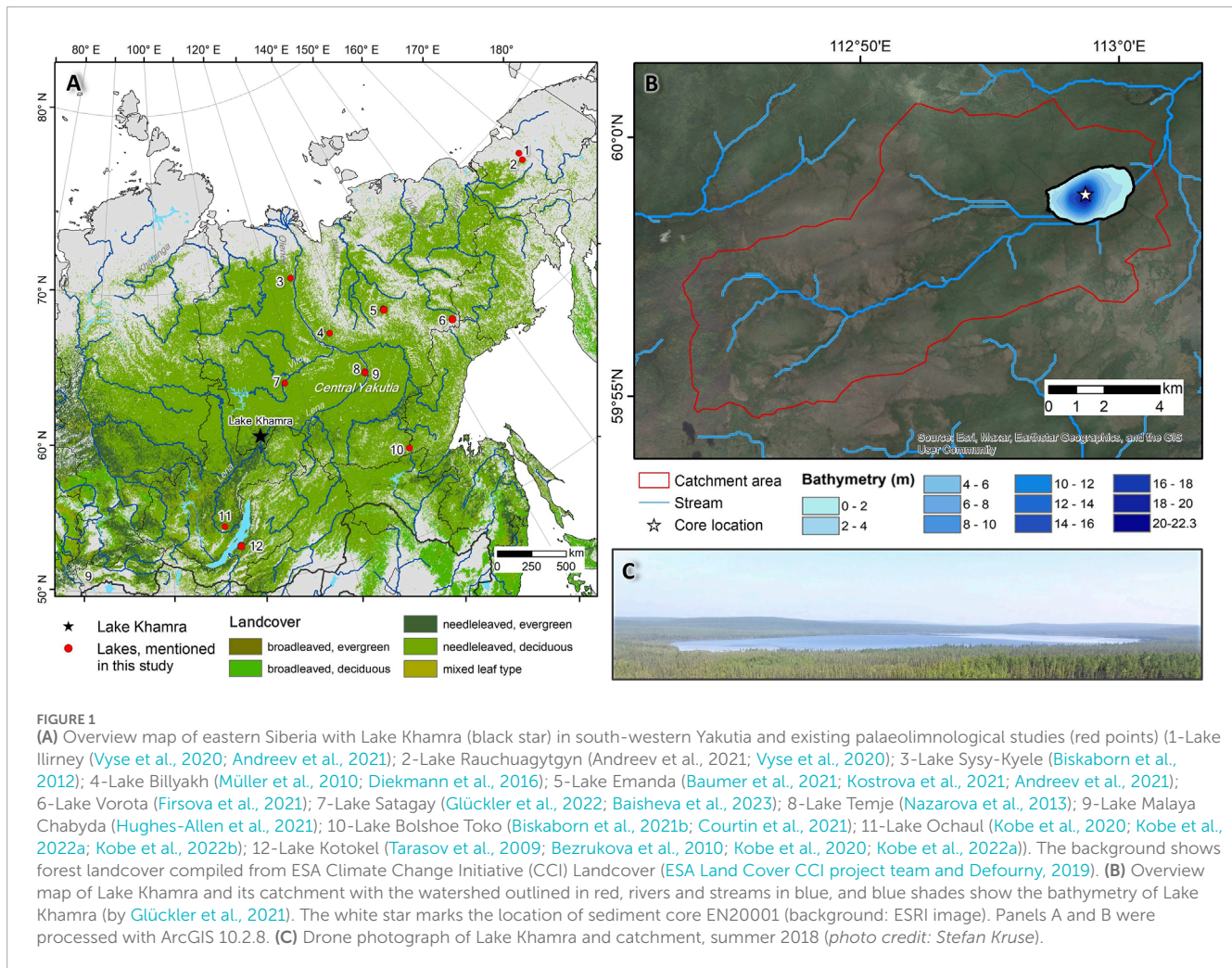
Future warming in northern Asia is predicted to result in widespread permafrost loss and related ecological change (Stuenzi et al., 2021; IPCC, 2022; Kruse and Herzschuh, 2022; Li et al., 2022), particularly in the southern permafrost and taiga areas such as south-western Yakutia. Yet, the long-term response of climate- and permafrost-sensitive vegetation and lake ecosystems in these areas is poorly understood, due to the limited number of suitable palaeoecological records (Kaufman et al., 2020; Herzschuh et al., 2022). Hence, our ability to predict future ecosystem dynamics is restricted.

Climate reconstructions indicate that Yakutia was drier around the Last Glacial Maximum (LGM, 21 cal ka BP; Binney et al., 2017; Tian et al., 2018; Pratap and Markonis, 2022) than at present and was covered by widespread steppe-tundra extending much farther south than the present tundra areas (Courtin et al., 2021). It is likely there were glacial refugia of taiga tree taxa but their locations are largely unknown. With the post-glacial warming, scarce *Betula* (birch)- and *Alnus* (alder)-rich woodland expanded (Andreev et al., 2002; Müller et al., 2010; Werner et al., 2010; Binney et al., 2017; Ashastina et al., 2018; Tian et al., 2018; Cao et al., 2019) and widespread *Larix* (larch) forests became established in Yakutia during the Holocene (Andreev et al., 2002; Schulte et al., 2022a). Since the late Mid-Holocene, *Pinus sylvestris* (Scots pine) expanded into these forests, particularly on sandy soils along the rivers (Troeva et al., 2010; Herzschuh et al., 2013; Tian et al., 2018). Regionally, *Picea* (spruce) also became more abundant reflecting a complex ensemble of drivers of forest composition including climate, fire, and permafrost (Herzschuh, 2020; Dallmeyer et al., 2022).

Sparse palaeolimnological records from Yakutia (Subetto et al., 2017) indicate that lake changes are sensitive to climate, vegetation, and permafrost change (Herzschuh et al., 2013; Biskaborn et al., 2016). However, most available records in the Yakutian lowlands originate from shallow thermokarst lakes which became established during the Early Holocene warming that triggered thermokarst activity (Biskaborn et al., 2012; Pestryakova et al., 2012). They are prone to desiccation and rapid shallowing (Ulrich et al., 2017). For example, different stages of thaw-lake (alaas lake; Crate et al., 2017) development could be traced using sedimentary ancient DNA (*sedaDNA*) diatom amplicon sequencing (Baisheva et al., 2023). Hence, the vast majority of studies from Yakutian lowlands cannot serve as a continuous archive of the last glacial period and subsequent Holocene development. Studies covering the Late Glacial are mainly from mountain regions in Yakutia and Chukotka. They mainly show glacial activity in the catchment during the Late Glacial and relatively stable Holocene conditions (Diekmann et al., 2016; Vyse et al., 2020; Andreev et al., 2021; Baumer et al., 2021;

Biskaborn et al., 2021b; Courtin et al., 2021; Firsova et al., 2021; Huang et al., 2021; Vyse et al., 2021; Andreev et al., 2022). Although these results may not be directly applicable to non-thermokarst, non-glacier impacted lowland lakes, these mountain lakes may actually better reflect the climate-driven environmental history.

Classic methods for palaeoenvironmental investigations from lake sediments are palynological analyses of pollen (Bennett and Willis, 2001) and non-pollen palynomorphs (van Geel, 2001). However, exploiting only pollen-based reconstructions has some limitations, as pollen types are often recorded only at genus level and can have broad preferences (Tarasov et al., 1998). Hence, integrating palynological methods with *sedaDNA* amplicon sequencing is a way to enhance the resolution and accuracy of taxonomic identification (Zimmermann et al., 2017a; Zimmermann et al., 2017b; Niemeyer et al., 2017; Parducci et al., 2017; Liu et al., 2020; Courtin et al., 2021; Courtin et al., 2022; Karachurina et al., 2023). *SedaDNA* amplicon sequencing using the P6 loop of trnL primers (Taberlet et al., 2007) provides rapid and accurate species identification in samples from lake sediments and permafrost and can reveal palaeo and modern catchment vegetation (Alsos et al., 2016; Alsos et al., 2018; Zimmermann et al., 2017a; Zimmermann et al., 2017b; Clarke et al., 2019; Crump et al., 2019; Giguet-Covex et al., 2019; Liu et al., 2020; Courtin et al., 2021; Courtin et al., 2022; Huang et al., 2021; Li et al., 2021; von Hippel et al., 2022; Glückler et al., 2022), as well as helping to reconstruct a lake's macrophytes and aquatic plants (Heinecke et al., 2017; Crump et al., 2019; Stoof-Leichsenring et al., 2022; Baisheva et al., 2023; Karachurina et al., 2023; Revéret et al., 2023). Modern and palaeo-reconstructions have revealed that macrophytes are sensitive to environmental changes such as climate warming and are responsive to changes in lake morphometry and chemistry (Heinecke et al., 2017; Stoof-Leichsenring et al., 2022) and are suitable for environmental reconstructions (Revéret et al., 2023). Additional information on lake development in Yakutia can be derived from diatoms (Battarbee et al., 2001), as they are excellent indicators of lake changes over time (Biskaborn et al., 2012; Pestryakova et al., 2012; Biskaborn et al., 2013a; Biskaborn et al., 2016; Pestryakova et al., 2018). Supplementing the morphological studies and *sedaDNA*, diatom amplicon sequencing using rbcL primers (Stoof-Leichsenring et al., 2012) is now a well-established method for tracing lake evolution (Evans et al., 2007; Stoof-Leichsenring et al., 2012; Stoof-Leichsenring et al., 2014; Stoof-Leichsenring et al., 2015; Dulias et al., 2017; Huang et al., 2020; Stoof-Leichsenring et al., 2020; Baisheva et al., 2023) as well as distinguishing possible sub-taxa (Dulias et al., 2017; Huang et al., 2020; Stoof-Leichsenring et al., 2020) and identifying intra-lake diversity (Biskaborn et al., 2019; Stoof-Leichsenring et al., 2020). Existing palaeolimnological reconstructions based on *sedaDNA* that combine aquatic and terrestrial ecosystem development are



beneficial, yet still sparse (Niemeyer et al., 2015; Klemm et al., 2016; Karachurina et al., 2023). Although challenges persist, additional research is essential to improve our understanding of historical changes of aquatic and terrestrial biodiversity shifts (Capo et al., 2021).

Here we investigate the aquatic and terrestrial ecosystem development in south-western Yakutia since the end of the LGM using a multiproxy approach to study sediments from Lake Khamra. We aim to reconstruct (i) lake ecosystem development, (ii) terrestrial ecosystem changes, and (iii) their relationships with climate dynamics.

2 Study site

Lake Khamra (59.990° N, 112.983° E) is located in the south-western Republic of Sakha (Yakutia), eastern Siberia, ca. 30 km north of the Lena River, at an elevation of 340 m a.s.l., in the Lensky District (Figure 1). The lake is 3.1 km long with a total surface area of 4.6 km² and a maximum depth of 22.3 m (Biskaborn et al., 2021a). The lake catchment area is 107.4 km² (Glückler et al., 2021), with an inflow stream supplying the lake from the west and one outflow from the lake at the eastern end of the lake.

The catchment of the lake is underlain by Cambrian bedrock of the near-Lena (Prilenskoye) plateau, part of the Siberian platform (Shahgedanova, 2002). More geological details are described in Glückler et al. (2021) after Chelnokova et al. (1988). It has a temperate, being relatively humid and warm despite being in the East Siberian continental province (Shahgedanova, 2002). The meteorological dryness index for this region ranges between 0.5 and 0.7, which is considerably humid for Yakutia, according to the Agricultural Atlas of Yakutia (Matveev, 1989). Annual precipitation is moderate, varying between 500 and 600 mm. Summer precipitation is 150–200 mm; in winter the snow depth can reach 80 cm (Matveev, 1989). Annual mean ground temperature at a depth of 10–20 m ranges between 0°C and 1°C (Shestakova et al., 2021), representing a transition from discontinuous to sporadic permafrost (Obu et al., 2019). Mean air temperature is 18°C for July and –40°C for January (Fedorov et al., 2018). The main climatic drivers in the region are the Arctic Oscillation (AO) and the North-Atlantic Oscillation (NAO) deduced from meteorological data (Wu and Wang, 2002; Wang et al., 2005) for the present climate. Air mass formation in the region occurs all-year-round (Woodwell and Mackenzie, 1995; Shahgedanova, 2002).

According to Isaev et al. (2010), the area is a subzone of the Middle Taiga forest, sub-province central Yakutian Middle Taiga. The lake lies

within the transition zone of evergreen to deciduous needle-leaf boreal forest (as described in [Glückler et al., 2021](#)). It is the northern border of the distribution area for three species: *Pinus sibirica*, *Abies sibirica*, and *Larix sibirica* ([Isaev et al., 2010](#)). The modern forest vegetation in the Lake Khamra region is mainly composed of deciduous *Larix gmelinii*, *Betula pendula*, *Salix* spp., and evergreen *P. sylvestris*, *P. sibirica*, *Picea obovata*, and *A. sibirica* ([Geng et al., 2022](#); [Miesner et al., 2022](#)).

3 Materials and methods

3.1 Fieldwork

Lake sediment cores were retrieved from Lake Khamra in spring 2020 from lake ice at a water depth of 20.6 m (59.99095° N, 112.98345° E). Coring was performed by repeated and overlapping extraction of six sediment cores with a diameter of 60 mm and composite depth capacity of ca. 10.8 m. A UWITEC tripod piston coring system fixed on the lake ice-cover was used to retrieve 3-m sections with 0.5 m overlaps. Five overlapping short cores with intact surface layers were retrieved with a UWITEC gravity corer. The sediment was protected in transparent PVC tubes. To protect the cores from freezing, heating and sunlight, the PVC tubes were cut into 1-m long parts and stored and transported in thermoboxes. After transportation to the Alfred Wegener Institute Helmholtz Centre for Polar and Marine Research, Potsdam in Germany (AWI-P) the cores were kept in cold and dark storage at 4°C until subsampling.

3.2 Laboratory analyses

3.2.1 Core processing

Opening of the core into working and archive parts and the subsampling of working halves took place in a clean environment at the German Research Center for Geosciences (GFZ) in a climate chamber at a temperature of 4°C. In order to restrict any possible contamination before and during the subsampling, all surfaces in the climate chamber and every tool and core tube were cleaned with DNA-Exitus (VWR, Germany) and deionised water, following [Epp et al. \(2019\)](#). Overall, 49 samples (2-cm slices) were taken from selected depths parallel to the layering in working halves of the cores. Outer edges of the sample slices were cut off and regarded as residue. Sediment material from the inner part was subdivided into subsamples for multiproxy analytical purposes, including samples for dating, measurements of total organic carbon (TOC) and total nitrogen (TN), pollen identification, and sedimentary ancient DNA (*seDNA*) amplicon sequencing of plants and diatoms. To avoid contamination risks, *seDNA* samples were prioritised in subsampling and were stored immediately at -20°C in the freezer of the palaeogenetic laboratory at AWI-P. Samples for other analyses were preserved in cold storage at 4°C. Archive halves of the core EN20001 were prepared for non-destructive scanning, to perform core splicing (define overlaps) and establish a composite depth for age-depth modelling.

3.2.2 Radiocarbon dating and age-depth modelling

Determination of age was conducted by the radiocarbon (^{14}C) method from 38 bulk sediment samples (1 cm thick) and analysed

by accelerator mass spectrometry with the Mini Carbon Dating System (MICADAS) at AWI in Bremerhaven, Germany. Age-depth modelling and interpolation was performed on mid-point composite values of ^{14}C samples ([Table 1](#)) using the R package 'Bacon' ([Blaauw and Christen, 2011](#)) and the IntCal20 calibration curve ([Reimer et al., 2020](#)). Calibration is based on years before present (cal yr BP, with 'present' as 1950 CE/AD). We used the ^{14}C values of the surface sample EN20003 to estimate the reservoir value (ΔR 1029.4 years) and the error (ΔR_{STD} 20.7 years). As well as the applied reservoir effect evaluation in the Bacon routine, a 1-cm hiatus was set at 921 cm. Modelled ages and 2-sigma uncertainties were interpolated to obtain mean ages and uncertainty intervals at every composite depth and to calculate mean sedimentation rates (SR; cm a^{-1}).

3.2.3 TOC and TN analyses

Total organic carbon (TOC) and total nitrogen (TN) were analysed in the sediment laboratory at AWI-P. Samples were freeze-dried and homogenised by grinding in a planetary mill. TOC was subsequently measured using a soliTOC cube analyser (Elementar Analysensysteme GmbH, Germany). TN was measured from freeze-dried samples using a TruMac CNS elemental analyser (LECO, Germany). Following [Meyers and Teranes \(2002\)](#), the percent per weight of TOC and TN was used to calculate the C/N ratio, which was then multiplied by the ratio of atomic weights of nitrogen and carbon (1.167) to yield C/N atomic ratios ($\text{TOC}/\text{TN}_{\text{atomic}}$; [Meyers and Teranes, 2002](#)).

3.2.4 XRF scanning for sediment geochemistry

XRF profile scanning was carried out using an AVAATECH X-Ray Fluorescence (XRF) Core Scanner at the Bundesanstalt für Geowissenschaften und Rohstoffe (BGR), Berlin, Germany. Before scanning, cores were cleaned, levelled, and covered with a 4 μ thin foil. Elements were measured using a rhodium metal X-ray tube at 10 kV with 0.75 mA, 13 s, with no-filter for the main elements, and 30 kV with 1.5 mA, 15 s, Palladium-thick filter for the minor elements. Compositional depth was derived using XRF data and radiocarbon data from the overlapping core sections. The scanning resolution was 1 cm between 0 and 659 cm and 729 and 1103 cm, and 0.5 cm between 659 and 729 cm, to test for fine laminations ([Supplementary Material](#)). Elements were assessed using the chi square (χ^2) statistic and those selected for this study are Zr (median χ^2 is 0.6), Br (median χ^2 is 0.75), Mn (median χ^2 is 0.5), and Fe (median χ^2 is 2.2).

3.2.5 Pollen analyses

A standard hydrofluoric acid (HF) technique was used for pollen preparation ([Berglund and Ralska-Jasiewiczowa, 1986](#)) in a pollen laboratory at AWI-P. A tablet of *Lycopodium* marker spores was added to each sample for calculating total pollen and spore concentrations, following [Stockmarr \(1971\)](#). Water-free glycerol was used for sample storage and preparation of the microscopic slides. Pollen and spores were identified at magnifications of $\times 400$ using published palynological keys and atlases ([Kupriyanova and Alyoshina, 1972](#); [1978](#); [Bobrov et al., 1983](#); [Reille, 1992](#); [Reille, 1995](#); [Reille, 1998](#)). In addition to pollen and spores (including ferns, mosses, clubmosses, spike moss, and a horsetail genus), a number of non-pollen palynomorphs (namely, fungi spores, remains of

TABLE 1 Radiocarbon ages from 38 bulk sediment samples from the Lake Khamra core. The depth refers to depth below the sediment surface.

Sample ID	Depth (cm)	¹⁴ C age (years)	Error (±)	¹⁴ C reservoir correction (years)	Sample ID	Depth (cm)	¹⁴ C age (years)	Error (±)	¹⁴ C reservoir correction (years)
AWI-7500.1.1	0 ^a	1029.4	20.7	- ^b	AWI-10462.1.1	744	6727.4	28	1029.4
AWI-7474.1.1	12	1481.1	23	1029.4	AWI-7504.1.1	750	6916.4	24	1029.4
AWI-7475.1.1	62	1389.8	21	1029.4	AWI-7490.1.1	766	6753.1	25	1029.4
AWI-7476.1.1	115	2072.8	21	1029.4	AWI-7491.1.1	814	7644.6	26	1029.4
AWI-7477.1.1	165	2528.5	22	1029.4	AWI-10463.1.1	849	8371.5	29	1029.4
AWI-7478.1.1	217	2983.1	23	1029.4	AWI-7492.1.1	861	8511.7	27	1029.4
AWI-7502.1.1	244	3239.5	22	1029.4	AWI-10464.1.1	875	8940.1	28	1029.4
AWI-7479.1.1	246	3277.2	22	1029.4	AWI-10465.1.1	893	10382.7	31	1029.4
AWI-7480.1.1	299	3561.3	22	1029.4	AWI-7493.1.1	909	10848.7	30	1029.4
AWI-7481.1.1	349	3652.3	22	1029.4	AWI-10466.1.1	921	11469.9	33	-
AWI-7482.1.1	401	4155.8	23	1029.4	AWI-10467.1.1	933	12019.6	32	-
AWI-7483.1.1	451	4654.3	23	1029.4	AWI-7494.1.1	959	12239.8	30	-
AWI-7503.1.1	472	4897.6	22	1029.4	AWI-7495.1.1	976	12928.9	31	-
AWI-7484.1.1	493	5174.6	23	1029.4	AWI-7505.1.1	981	12934.1	30	-
AWI-7485.1.1	545	5600.1	24	1029.4	AWI-10468.1.1	1004	13098.6	33	-
AWI-7486.1.1	593	6183.8	25	1029.4	AWI-2043899	1026	13952.1	32	-
AWI-7487.1.1	643	5926.1	25	1029.4	AWI-7496.1.1	1042	14856.1	39	-
AWI-7488.1.1	692.5	6323.7	24	1029.4	AWI-10470.1.1	1058	12351.1	33	-
AWI-7489.1.1	716	6661.3	24	1029.4	AWI-7497.1.1	1076	16360.5	38	-

^aSurface sample (EN20003) has been dated to estimate the reservoir value (Supplementary Material).

^bIn the model, depth 0 was set to the date of sampling.

algae and invertebrates) were identified when possible and counted (van Geel, 2001 and references therein).

An average of 309 pollen grains (minimum 178, maximum 377) was counted per sample. The relative percentages were calculated based on the total sum of pollen taxa (Supplementary Material); spore percentages on the sum of pollen and spores; the relative percentages of fungal spores on the sum of the pollen and fungal spores; and the relative percentages of algal remains from the sum of pollen and algae remains.

3.2.6 SedaDNA analyses

All steps from DNA extraction to polymerase chain reaction (PCR) set-up were performed in a dedicated palaeogenetic laboratory at AWI-P. For each extraction batch, one extraction blank was added to control for the general cleanliness of the extraction procedure and putative contamination in the DNA extraction chemicals. For the PCR preparation step, No Template Controls (NTCs) were added to control for chemical contamination of PCR chemicals. DNA extractions were performed using the Dneasy PowerSoil Max DNA Isolation Kit (Qiagen, Germany) with 2.2–6.8 g sediment input, following Epp et al. (2019). Extracted *seda*DNA was combined and concentrated with the GeneJet PCR Purification Kit (Thermo Scientific, United States). The concentrated DNA was quantified with a broad range dsDNA Assay Qubit Fluorometer (Invitrogen, United States) and DNA was diluted to 3 ng μL^{-1} for initial input into the PCR reactions.

For the PCR set-up, we included 3 μL of taxon-specific primers (1 μL each), 0.25 μL of Platinum™ Taq High Fidelity DNA Polymerase and buffer (Invitrogen, United States), 10x HiFi buffer (2.5 μL), dNTPS (2.5 μL), Bovine Serum Albumin (1 μL ; VWR, Germany), MgSO_4 (1 μL), and 12.75 μL of DEPC water (VWR, Germany). We used standard primers targeting the chloroplast trnL P6 loop (Taberlet et al., 2007) for the amplification of vascular plants and primers diat_rbcL705 and diat_rbcL808 (Stoof-Leichsenring et al., 2012) for the amplification of diatoms. All primers were modified with an NNN-8bp tag to establish sample multiplexing. PCRs for plant and diatom amplicon sequencing approaches were run in three replicates.

PCR products were amplified using a Biometra ThermoCycler (Biometra, Germany) at initial denaturation at 95°C for 5 min, followed by PCR cycles with denaturation at 95°C for 30 s, annealing at 50°C for 30 s, and elongation at 68°C for 30 s. For the amplification of plant DNA, we used 40 cycles, and 50 cycle PCRs were run for the amplification of diatom DNA. PCR success was checked by gel electrophoresis using 2% agarose gels and visualisation with the gel documentation system Geldoc GO Imaging (Bio-Rad, Germany).

Purification of PCR products for each independent run was done with MinElute (Qiagen, Germany), following the manufacturer's protocol. PCR products were pooled equimolarly and were finally concentrated to about 1000 ng DNA in 30 μL . Finally, two PCR sample pools were prepared and were sent to Fasteris (Genesupport, Fasteris SA, Switzerland) for preparing a PCR-free library (using the metafast protocol) and amplicon sequencing in paired-end mode (2x 150 bp) on an Illumina NextSeq 500 platform (Illumina Inc.) resulting in the runs APMG60 (for diatoms) and two independent runs APMG-39 and APMG-64 (for plants).

3.2.7 Amplicon sequencing and taxonomic assignment

After Illumina amplicon sequencing, datasets of diatom and plant composition were processed using OBITools3 (<https://git.metabarcoding.org/obitools/obitools3>) following the bioinformatic pipeline given in Boyer et al. (2016). To align forward and reverse reads, data were combined using the “*obi alignpairedend*” command, and to remove unpaired reads “*obi grep*” was used. To allocate reads to the corresponding combinations of primer tags the command “*obin gsfiler*” was used. Grouping and counting of identical sequences was performed using “*obi uniq*”. Denoising data using “*obi annotate*” removed sequences with <10 counts and <10 length (base pairs). The taxonomic assignment was conducted using different databases. The Diatom EMBL reference database was built by applying “*obie copcr*” with diatom primers on the EMBL Nucleotide Sequence Database (Release 143 April 2020). Ecopcr results were then converted with “*build_ref_db*” into an OBITools diatom database that “*obi ecotag*” uses for taxonomic classification (Baisheva et al., 2023). Plant DNA sequences were matched against the customised database for Siberian plants “SibAla_2023”. The compilation of the database was done using different R packages with the following steps (Courtin et al., 2024¹): 1. Taxa with >10 occurrences were selected from a given region (55–90°N, 50–150°E and 40–90°N, 150°E–140°W) using the Global Biodiversity Information Facility (GBIF, 2023) resulting in 233 families, 1059 genera, and 4849 species. 2. Available P6 loop sequences from public DNA databases (arctorbryo: Sønstebo et al., 2010; Willerslev et al., 2014; Soininen et al., 2015; EMBL 143; Kanz et al., 2005; PhyloNorway; Alsos et al., 2022) were used to extract references sequences from the selected GBIF taxa. 3. Additional P6 loop references of plants which were not in the GBIF data, but present in the distribution area, confirmed by using the Plants of the World Online (2023) database (<https://powo.science.kew.org/>) were added. 4. A quality filtering of the finally selected P6 loop sequences was performed. 5. Conversion of the sequences into an OBITools3 database. The final SibAla_2023 database compared with given occurrences in GBIF amounts to 95.7% (family level), 89.4% (genus level), and 70.1% (species level) of taxonomic coverage. Finally, the SibAla_2023 database includes 4939 entries, comprising 3398 species, 947 genera, and 223 families that collapse into 2371 unique P6 loop sequence types.

The taxonomic assignment of diatoms was based on a 98%–100% similarity threshold against the references in the OBITools diatom database. Results from the OBITools pipeline of the diatom dataset were further filtered at the level of amplicon sequence variants (ASVs). ASVs not belonging to Bacillariophyta (diatoms) were discarded.

For plant amplicon sequencing, datasets from two independent runs (APMG-39 and APMG-64) were first merged, and only sequences with 100% matches to the SibAla_2023 database were included in the final analysis. Amplicon sequencing of plant *seda*DNA sequencing yielded 25,263,993 counts (Supplementary Material), of which the majority (77.6%) belong to aquatic plants, while terrestrial plants constitute 20.3%, and the remaining

1 Courtin, J., Stoof-Leichsenring, K. R., Lisovski, S., Alsos, I. G., Biskaborn, B. K., Diekmann, B., et al. (2024). Potential plant extinctions with the loss of the Pleistocene mammoth-steppe. Nat. Commun. In review.

1.7% belong to control blanks and other taxa sequenced to a coarser taxonomic level (e.g., clade, North American clade, Apiooid superclade). Output data were separated into two databases (terrestrial plants and aquatic plants).

Finally, each dataset was rarefied to the minimum number of counts (diatoms $n=7298$; aquatic plants $n=5307$; and penultimate least number for terrestrial plants $n=2291$) to normalise the datasets prior to subsequent statistical analyses (Supplementary Material). The rarefaction process was repeated 100 times and the mean value calculated (Kruse, 2021). Diatoms and plants were assigned to “scientific names” (highest taxonomic level possible).

3.2.8 Statistics

Statistical analyses of the obtained results and visualisations were completed in R, version 4.3.1 (R Core Team, 2023). Relative abundances from counts of *sedaDNA* diatoms, terrestrial plants, and macrophytes were calculated using the package ‘*vegan*’ (Oksanen et al., 2022). All stratigraphic plots were done using the package ‘*rioja*’ (Juggins, 2022), function “strat.plot”. The obtained elemental compositional data from XRF scanning were given in counts per second (cps). XRF transformations were needed to normalise the data. Single element values were transformed with a centred-log ratio (clr) transformation, while for ratios of elements, an additive-log ratio (alr) transformation was applied using the package ‘*compositions*’ (van den Boogaart et al., 2023). Principal component analysis (PCA) was used to illustrate the compositional change in a bio-proxy’s relationship in lacustrine and terrestrial environments and to assess the impact of biogeochemical datasets. All steps of the ordination analyses were performed with the ‘*vegan*’ R-package (Oksanen et al., 2022). Log-transformed relative proportions for *sedaDNA*, pollen data, and selected clr and alr transformed XRF and square-rooted TOC and TOC/TN_{atomic} values were plotted via “*envfit*” onto the PCA ordination calculated with the “*rda*” function.

4 Results

4.1 Core lithology and chronology

The sedimentary sequence of core EN20001 is defined by four lithological units (LU1 to 4, Figure 2B). The basal section LU1 (1076–1067 cm) consists of organic-poor coarse ‘sandy’ minerogenic material. LU2 (1067–1052 cm) is characterised by the presence of fine dark organic-rich layers embedded within coarse ‘sandy’ organic-poor minerogenic material. LU3 (1052–892 cm) is composed of a dark-grey organic-poor mixture of fine and medium-coarse material. LU4 (892–0 cm) is composed of a homogeneous organic-rich fine material of dark-brown colour and is similar to the lithology of the previous study from Lake Khamra (Glückler et al., 2021).

A reservoir effect occurs with the incorporation of pre-aged (old, ¹⁴C-depleted) carbon into sediments resulting in erroneously old radiocarbon dates (Philippsen, 2013). The modern reservoir effect was estimated to be 1029 years from dating of the total organic matter in a surface sample (Supplementary Material). We assume that this reservoir effect originates from the long water retention time in a big lake (Hendy and Hall, 2006). Furthermore, Glückler et al. (2021) previously discussed the lake’s reservoir effect as a result of the input of old organic carbon from the degrading permafrost landscape.

Accordingly, we corrected the obtained radiocarbon dates between the surface and 920 cm, and established an age-depth model based on the corrected ¹⁴C dates (Table 1). This interval equals the period of a deep lake according to our Mn/Fe record (see below). The reservoir effect correction was not applied to the lower part of the core (1076–921 cm) because for this interval we assume that sedimentation occurred in an ephemeral pond (as inferred from our proxy data, see below) characterised by short water-retention time and low TOC and Br (Figures 3C, D). To account for this shift when setting up the age-depth model, we inserted a 1-cm “hiatus” at 921 cm to artificially delete the memory. This step serves to best align the age-depth model with the recorded proxy data.

The model based on 38 radiocarbon dates (Table 1) shows a linear chronology (Figure 2A) and reveals that the samples in LU1 (1076–1068 cm) accumulated between 19.6 and 19.2 cal ka BP (max. 19.6 cal ka BP, min. 18.7 cal ka BP), LU2 samples (1068–1052 cm) accumulated between 19.2 and 18.4 cal ka BP (max. 19.2 cal ka BP, min. 18.01 cal ka BP), LU3 (1052–892 cm) spans from 18.4 to 10.5 cal ka BP (max. 18.4 cal ka BP, min. 10.49 cal ka BP), and LU4 (892–0 cm) from 10.5 cal ka BP to 2020 CE (max. 10.47 cal ka BP, min. –72 cal ka BP). The mean 95% confidence range for the core is 366 years (min. 28 years at 0 cm depth, max. 1273 years at 1060 cm depth). Median sedimentation rates (SR) are high within LU4 at 0.11 cm a^{–1} (Figure 3A), with the highest SR of 0.33 cm a^{–1} is observed at ca. 5.6 cal ka BP. SR in the older LUs are lower, being 0.02 cm a^{–1} for LU2 and 0.03 cm a^{–1} for LU3 and LU1. The core chronology for the upper 242 cm is in good agreement with the previous study of the Lake Khamra sediments (Glückler et al., 2021).

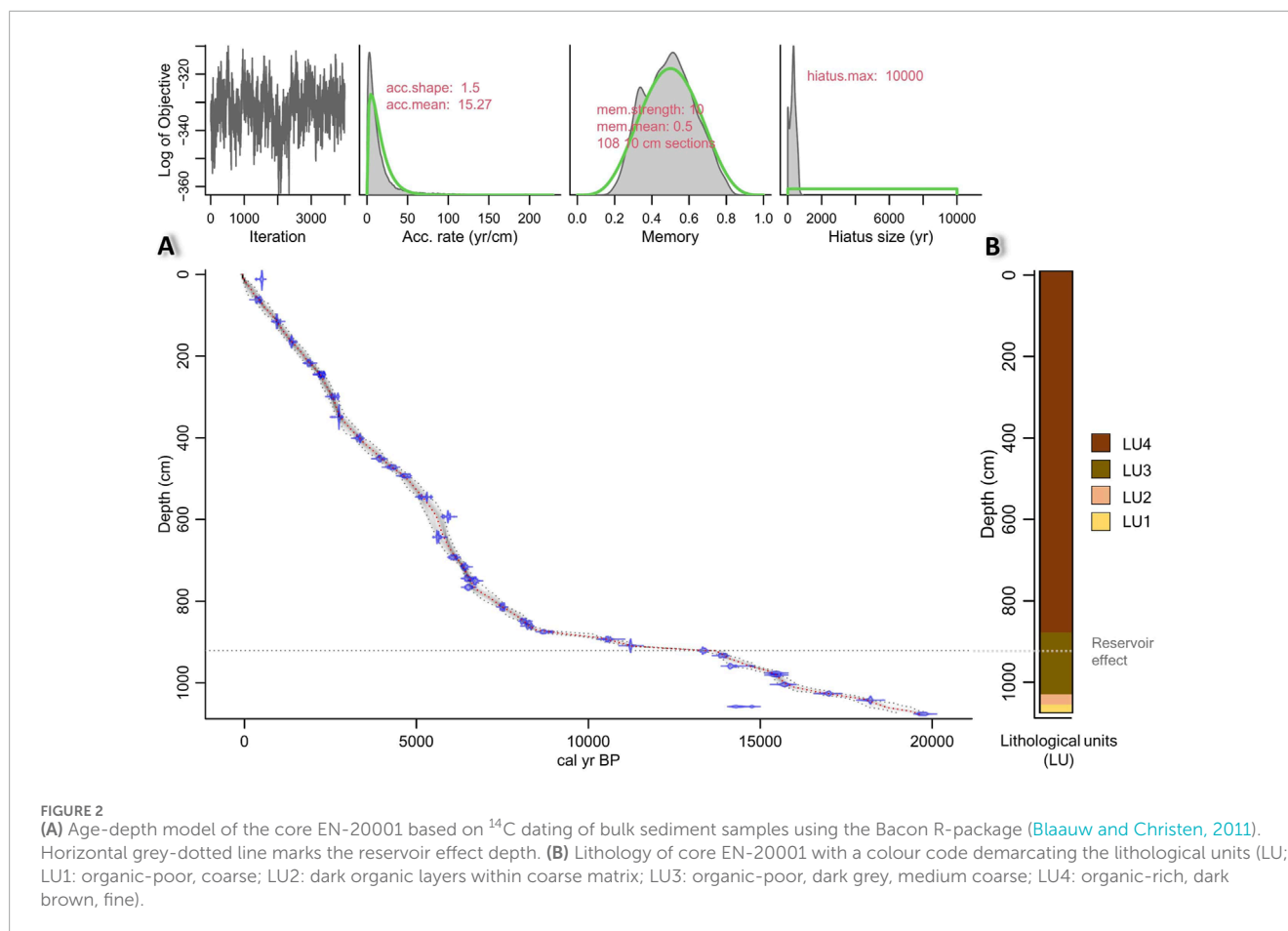
4.2 Biogeochemical core composition

The lowest TOC content (1.1 wt%) is found in LU1 (1076 cm, 19.6 cal ka BP). A TOC peak of 9.4 wt% occurs in LU2 at 1058 cm (18.6 cal ka BP) (Figure 3C). Consistently low values with a median of 4 wt% characterise LU3 from 18.4 to 10.6 cal ka BP. LU4 is characterised by a higher TOC content of 18.6 wt% and contains the highest TOC content (29.1 wt%) peaking at 814 cm (7.5 cal ka BP). The LU1 sample has a TOC/TN_{atomic} ratio of 9.2 (Figure 3E). LU2 and LU3 both have a median ratio of 12.5, while LU4 has high variability of between 14.3 and 10.3. XRF-derived Br (clr) reaches a maximum of Figure 3D in LU4 at 777 cm (6.8 cal ka BP) and its lowest value of –4.7 in LU1 at 1071 cm (19.4 cal ka BP). Br (clr) shows similar dynamics to TOC across all lithological units. XRF-derived Zr (clr) has high and quite constant values for LU1 to Figure 3B with a maximum of 1.5 at 948 cm (14.4 cal ka BP) and low values in LU4 with a minimum of –0.7 at 382 cm (3.1 cal ka BP). Mn/Fe (alr) shows highest values in Figure 3F with a maximum of –2.9 at 1070 cm (19.4 cal ka BP). In LU2 to LU4, Mn/Fe fluctuates between –3.2 and –5.2 and has low values of below –4.7 between 928 and 855 cm in LU3 and LU4 (13.8–8.2 cal ka BP).

4.3 Lake ecosystem proxies

4.3.1 Diatom *sedaDNA* amplicon sequencing

Diatom amplicon sequencing analyses of *sedaDNA* yielded 1,281,591 counts, of which only three counts belong to blanks (Supplementary Material). Final counts from the 25 samples resulted



in 1,281,588 counts, with a median of 43,516 counts per sample. 257 ASVs are grouped into 45 taxa at the highest taxonomic level possible, comprising family (3 taxa), genus (13 taxa), and species (29 taxa). The maximum number of counts (172,257) occurs in the sample from 6.4 cal ka BP (716 cm), while the minimum number of counts (7298 counts) occurs in the sample from 14.7 cal ka BP (959 cm). Only one amplicon was assigned from the lowermost sample at 19.6 cal ka BP (1076 cm), but at 94%.

SedaDNA diatom analyses (Figure 4) yielded 45 taxa with occurrences restricted to LU3 and LU4, comprising 16 benthic taxa, 15 epiphytic taxa, and 14 planktonic taxa. In LU3, there is a compositional change of epiphytic and planktonic diatom abundance. The epiphytic diatom *Pseudostaurosira elliptica* is the sole diatom recorded at 17 cal ka BP (1026 cm), and the unclassified *Staurosira* is the only and abundant epiphytic diatom at 14.7 cal ka BP (959 cm), constituting 84% of relative abundance. Planktonic *Aulacoseira* sp. and *A. granulata* first appear at 14.7 cal ka BP (959 cm), albeit at low abundance, making up 16%. *Aulacoseira* is dominant at 11.2 cal ka BP (909 cm) with a proportion of 99%. In LU4, diatom composition can be divided into three subzones according to relative changes between epiphytic and planktonic taxa.

LU4-1 (8.3–6.1 cal ka BP, 861–693 cm) is dominated by abundant epiphytic taxa (median 99.8%), while planktonic taxa have a median abundance of 0.2%, and benthic taxa first occur in this subzone. Epiphytic taxa are represented by abundant unclassified *Staurosira* with a maximum of 72%, *P. elliptica* with

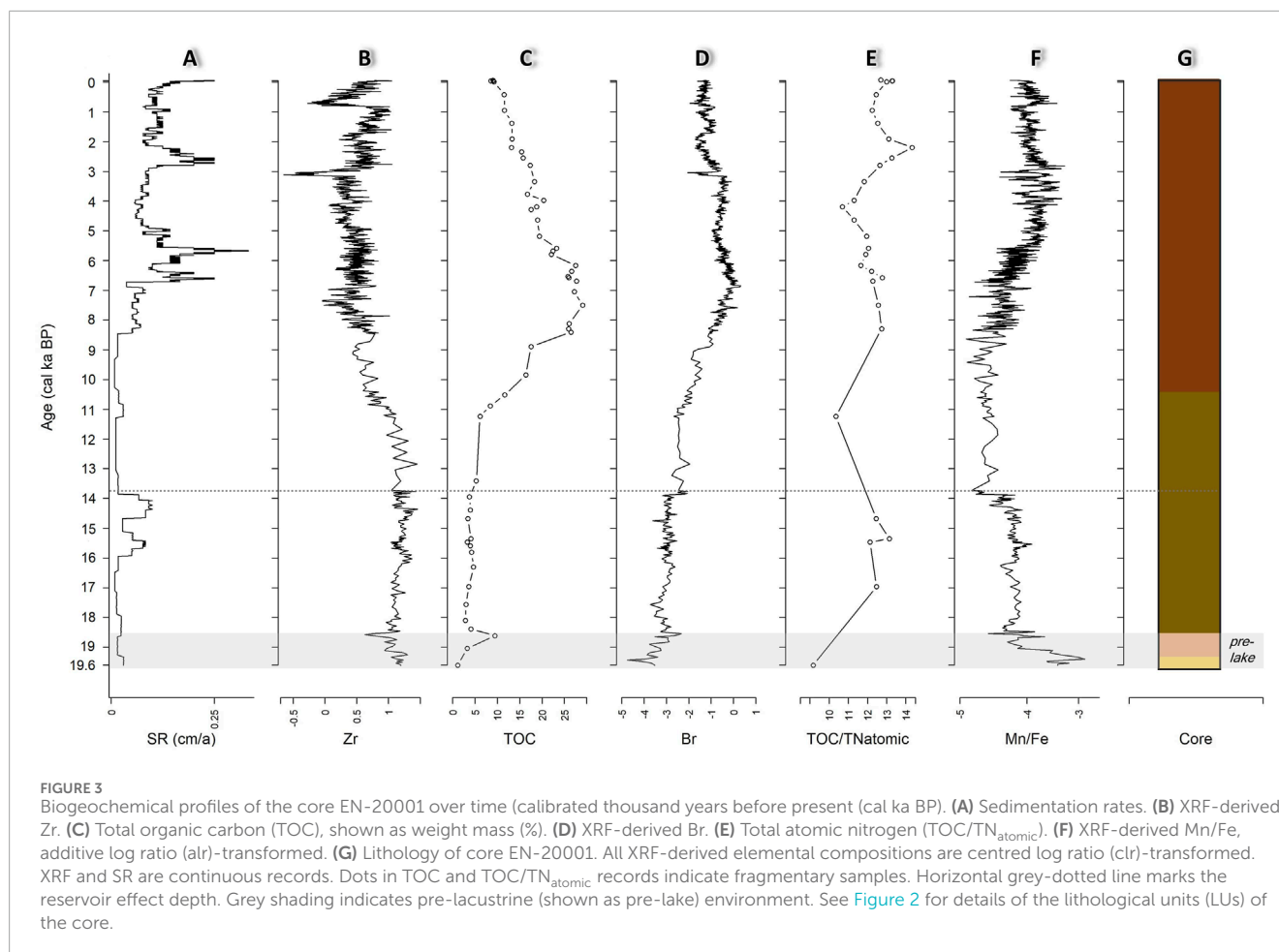
a maximum of 40%, and *Staurosirella martyi* with a maximum of 24%. The planktonic assemblage constitutes *Aulacoseira granulata* var. *angustissima* at up to 12%. Benthic *Pinnularia* is present at 7.5 cal ka BP (816 cm) with a maximum of 7%.

LU4-2 (5.8 cal ka BP to 3.3 cal ka BP, 643–401 cm) is dominated by planktonic taxa (median 69.6%), epiphytic taxa account for a median abundance of 29.6%, and benthic taxa make up a median of 0.9%. Dominant planktonic diatoms are *A. granulata* with a maximum of 59%, *Aulacoseira* up to 47%, *Stephanodiscus* up to 12%, and *Stephanodiscaceae* with a maximum of 11%. Epiphytic taxa are represented by *P. elliptica* (33%) and unclassified *Staurosira* (37%). Benthic taxa are only present at low abundances.

LU4-3 (2.8 cal ka BP to 1997 CE, 349–6 cm) is dominated by epiphytic diatoms at a median abundance of 84.4%, while planktonic taxa reach a median of 15.1%, and benthic taxa a median of 0.1%. Epiphytic taxa are represented by abundant *P. elliptica* with a maximum of 94%, *Tabellaria flocculosa* with a maximum of 33%, and unclassified *Staurosira* with a maximum of 17%. The planktonic assemblage is principally comprised of *Aulacoseira* up to 21%. Benthic taxa are present at lower abundance.

4.3.2 Macrophyte sedaDNA amplicon sequencing

The final aquatic plants dataset from the 49 samples contains 19,628,743 counts, with a median of 396,345 counts per sample, and 94 ASVs which are grouped into 65 taxa at the highest taxonomic level possible, comprising family (2 taxa), subfamily (2



taxa), genus (19 taxa), subgenus (4 taxa), and species (32 taxa). The maximum number of counts (1,246,647 counts) occurs in the sample from 2.3 cal ka BP (267 cm), while the minimum number of counts (5,307 counts) occurs in the lowermost sample from 19.6 cal ka BP (1076 cm).

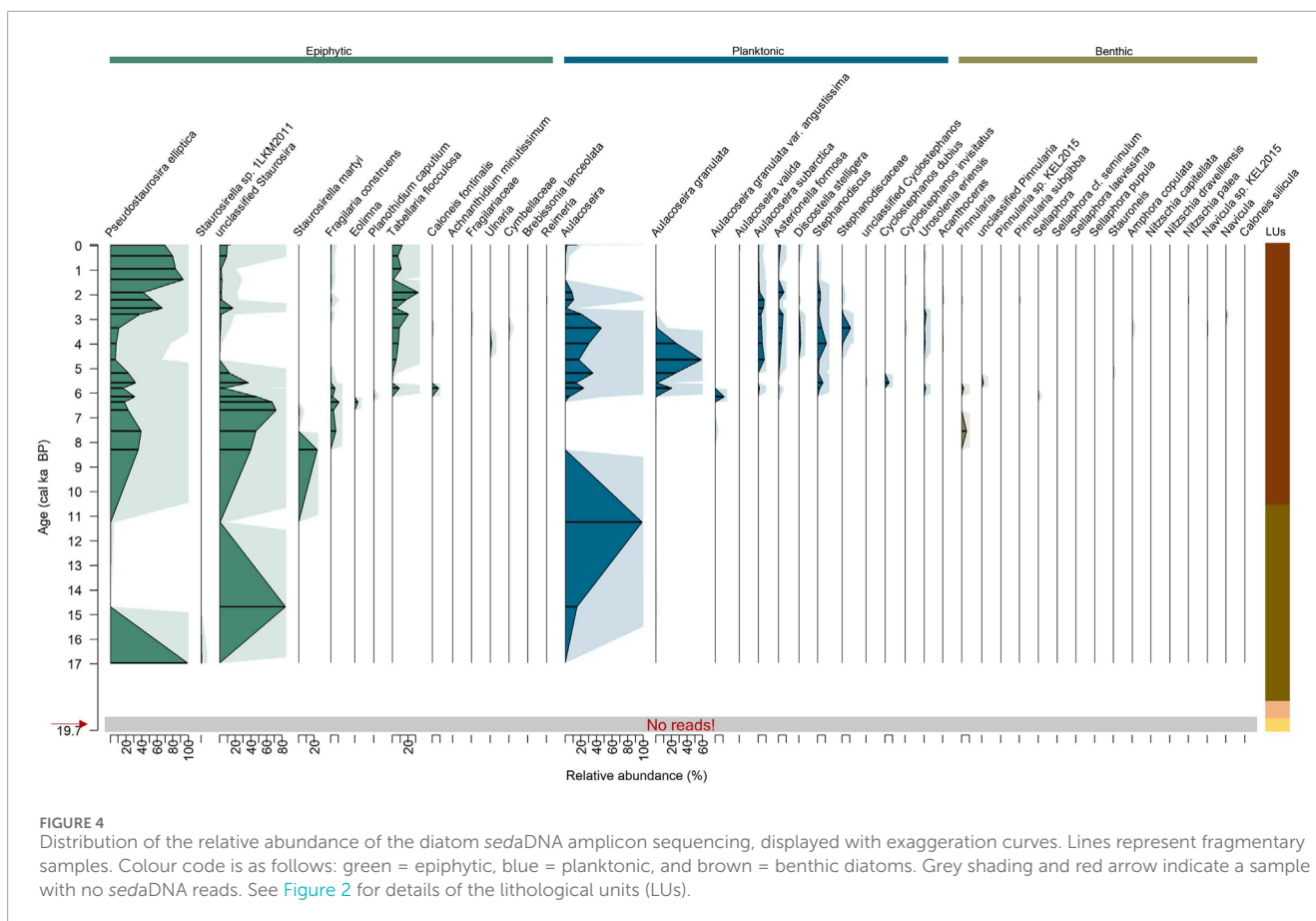
The aquatic and wetland plants (Figure 5) include one submerged-emergent, nine floating, 12 submerged, and 43 emergent taxa. The oldest sample at ca. 19.6 cal ka (1074 cm) in LU1 is primarily characterised by emergent wetland plants, with 72% of the total share, including *Veronica* subg. *Pseudolysimachium* (40%), *Equisetum* (19%), *Caltha palustris* (12%), and the single submerged taxon *Myriophyllum* (21%).

LU2 covers two samples at 19.1 cal ka BP (1066 cm) and at 18.6 cal ka BP (1058 cm), mainly characterised by submerged macrophytes and subdominant floating macrophytes. Dominant taxa in LU2 are *Potamogeton* with a median of 51.3% and *Ceratophyllum demersum* with a median of 21.2%. Emergent plants constitute an abundance below 10%.

LU3 spans from 18.4 until 10.6 cal ka (1051–894 cm) and is dominated by submerged plants with a median abundance of 55.9%. Submerged taxa include *Potamogeton* with a maximum of 83%, *Stuckenia* up to 25%, *P. praelongus* up to 24%, and *S. pectinata* up to 11%. Floating taxa make up a median of 23.7%, mainly consisting of *C. demersum* with a maximum of 60%. Emergent plants make up a median of 12.6%, where the

dominant taxon is *Callitriche hermaphroditica* with a maximum of 19%. Uniquely within this LU, the submerged-emergent taxon *Hippuris* occurs at 18.4 cal ka BP and is prominent with a maximum of 17%.

Macrophytes of LU4-1 spanning 9.8 to 7.1 cal ka BP (885–787 cm) are dominated by submerged taxa, with a median abundance of 67.6%. Submerged taxa include abundant *Potamogeton* at up to 79% and *P. praelongus* up to 39%. Floating taxa median abundance is 21.3%, mainly consisting of *C. demersum* with a maximum of 37%. Emergent plants make up a median of 9.1%. LU4-2 covers a period from 6.7 cal ka BP to 2.2 cal ka BP (766–246 cm) with a taxonomic composition characterised by emergent wetland plants with a median of 45.5% and submerged taxa with 37.6% of total share. Floating taxa make up a median of 10.4%. Emergent wetland plants include *C. hermaphroditica* at up to 45%, *Menyanthes trifoliata* up to 43%, and *C. palustris* up to 14%. Submerged taxa composition comprises *Potamogeton perfoliatus* with a maximum of 63.5%, *Potamogeton* with a maximum of 59%, and *P. praelongus* up to 24%. Floating taxa include *C. demersum* with a maximum of 74% and Nymphaeaceae with a maximum of 17%. LU4-3 spans from 1.9 cal ka BP to 1997 CE (217–6 cm) and is represented by submerged taxa with a median of 65.1%, mainly *Potamogeton* at up to 57% and *P. perfoliatus* up to 55%. Floating taxa with a median of 22.2% mainly comprise Nymphaeaceae with a maximum of 48%.



4.4 Terrestrial vegetation

4.4.1 Terrestrial plant *sedaDNA* amplicon sequencing

The final terrestrial plants dataset from the 49 samples contains 5,197,700 counts, with a median of 67,553 counts per sample, and 235 ASVs which are grouped into 191 taxa at their highest taxonomic level possible, comprising tribe (11), subtribe (2), family (5 taxa), subfamily (1 taxon), genus (76 taxa), subgenus (1 taxon), and species (87 taxa). The maximum number of counts (486,380 counts) occurs in the sample at 19.1 cal ka BP (1066 cm) and the minimum number of counts (105 counts) occurs in the sample at 8.3 cal ka BP (861 cm).

Terrestrial plant data consist of eight trees, 14 shrubs, 16 semi-shrubs, 12 grasses, 127 forbs, five ferns, and seven mosses and club mosses (Figure 6). The lowermost sample at ca. 18.4 cal ka BP (1076 cm) in LU1 is equally dominated by forbs (37%), shrubs (32%), and sub-shrubs (31%). The most abundant taxa are *Dryas* (sub-shrub) at 32%, Salicaceae (= *Salix*, shrub) at 30%, and Potentilleae at 28% (forb) likely *Potentilla acaulis* and/or *P. anserina*.

The two LU2 samples at 19.1 cal ka BP (1066 cm) and 18.6 cal ka BP (1058 cm) are dominated by shrubs with a median abundance of 88%, including Salicaceae (*Salix*) ranging between 57% and 69% and *Betula* ranging between 15% and 30%. The median proportion of forbs and sub-shrubs decreases in LU2. First reads of tree taxa—*Picea*,

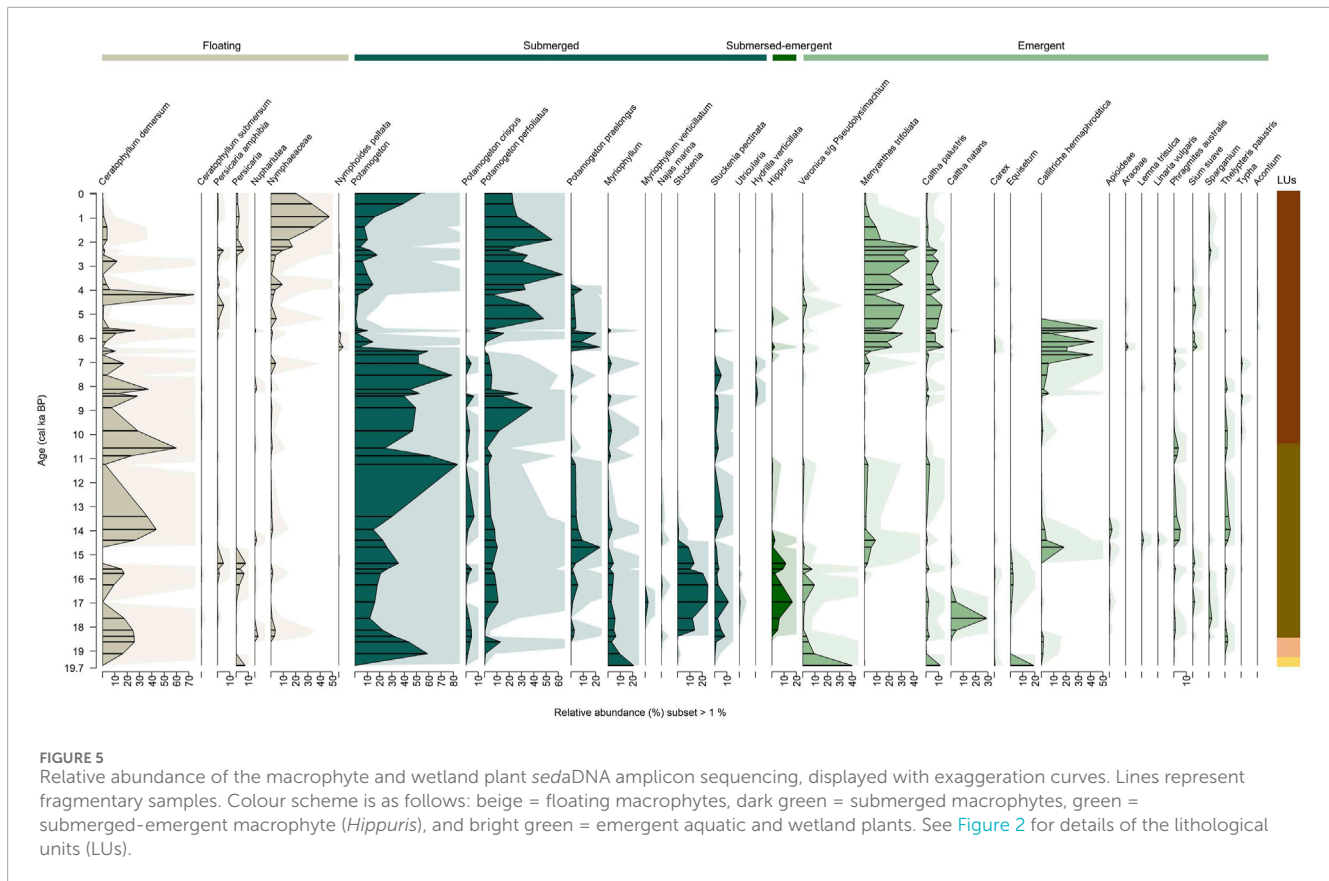
Pinus, and *Populus* (namely, *Populus tremula*) – occur in these two LU2 samples.

LU3-1 from 18.4 to 14.7 cal ka BP (1051–959 cm) is dominated by shrubs (median 70%) alongside forbs (median 23%). Dominant shrubs include Salicaceae (63%) and *Betula* (23%). Forbs include *Ranunculus* (at up to 10% of the total share), Asteraceae (up to 9%), and *Dryas* (up to 6%). Tree taxa are present but still not abundant. LU3-2 from 14.4 to 10.6 cal ka BP (949–894 cm) is similarly dominated by shrubs (median 65%) alongside forbs (median 28%). The dominant shrub is *Alnus* (up to 41%) although Salicaceae has a maximum of 80%. Within this subzone, tree abundance increases (8%), with *Populus* as the dominant tree taxon (up to 19%) and *Abies*, likely *A. sibirica*, occurring.

LU4 plant composition from 9.8 cal ka BP to 1994 CE (885–6 cm) is represented by 31 samples and contains abundant shrubs (median 54%), forbs (20.9%), sub-shrubs (8.7%), and trees (7.2%). Dominant shrubs are *Betula* (23%) and *Alnus* (16%). Salicaceae abundance decreases (4.6%). Dominant trees are *Larix* (with a maximum of 93%) peaking at 8.3 cal ka BP (861 cm), *Populus* (up to 60%), and *Picea* (up to 20%). Within this LU, the fern *Matteuccia struthiopteris* (up to 19%) occurs as well as *Alnus alnobetula* (= *Alnus fruticosa* or *Duschekia fruticosa*; up to 3%).

4.4.2 Pollen assemblages

In total, 32 pollen taxa were identified from 48 samples (Figure 7), composed of twelve arboreal pollen taxa (AP, six trees and



six shrubs and sub-shrubs) and 20 non-arboreal pollen taxa (NAP, 2 forbs and 18 graminoids). Pollen composition of LU1 at ca. 19.6 cal ka BP (1076 cm) mainly consists of NAP (92%). NAP in this sample is mainly Cyperaceae (68%) and Poaceae (18%). The highest share of forbs is of Brassicaceae (maximum 3%). The total share of AP is small (8%) including *Picea*, *Pinus* subg. *Haploxylon*, *Larix*, *Betula* sect. *Nanae*, and *Salix*.

In LU2, between ca. 19.1 and 18.6 cal ka BP (1066–1058 cm) the share of NAP taxa decreases to a median of 78%, while the median share of AP taxa increases to 22%. Abundant NAP taxa include Cyperaceae and Poaceae, with medians of 47% and 20%, respectively. The highest share of forbs is of *Artemisia* and Asteraceae, with a maximum of 5% and 4%, respectively. The most prominent AP taxa include the sub-shrub *Betula* sect. *Nanae* with a median of 13% and *Salix* with a median of 5%. Other AP taxa are not abundant—*Picea* (median 0.3%), *Pinus* subg. *Haploxylon* (0.3%), and *Larix* (0.6%).

In LU3 between 18.4 and 10.6 cal ka BP (1051–894 cm) pollen composition changes markedly from NAP dominated (median 16%) to AP dominated (median 84%). AP taxa are dominated by the sub-shrub *Betula* sect. *Nanae*-type with a median of 47% and a tree taxon *B.* sect. *Albae*-type with a median of 16%. *Larix* is present throughout (median 2.4%), while *Pinus* subg. *Haploxylon* (0.9%) and *Picea* (0.6%) have very low abundances. At the end of LU3, at 10.6 cal ka BP (894 cm), the abundance of *B.* sect. *Albae*-type increases sharply, constituting 49% and *Picea* increases up to a maximum of 23.7%. *Alnus fruticosa* (*alnobetula* ssp.) increases from 14.7 cal ka BP (959 cm) and peaks at 13.9 cal ka BP (933 cm) with a maximum of

10.7%. *Salix* is rather stable throughout with a median abundance of 3.5%. NAP taxon Cyperaceae decreases to a median of 24.7% and Poaceae drops to 6.3%.

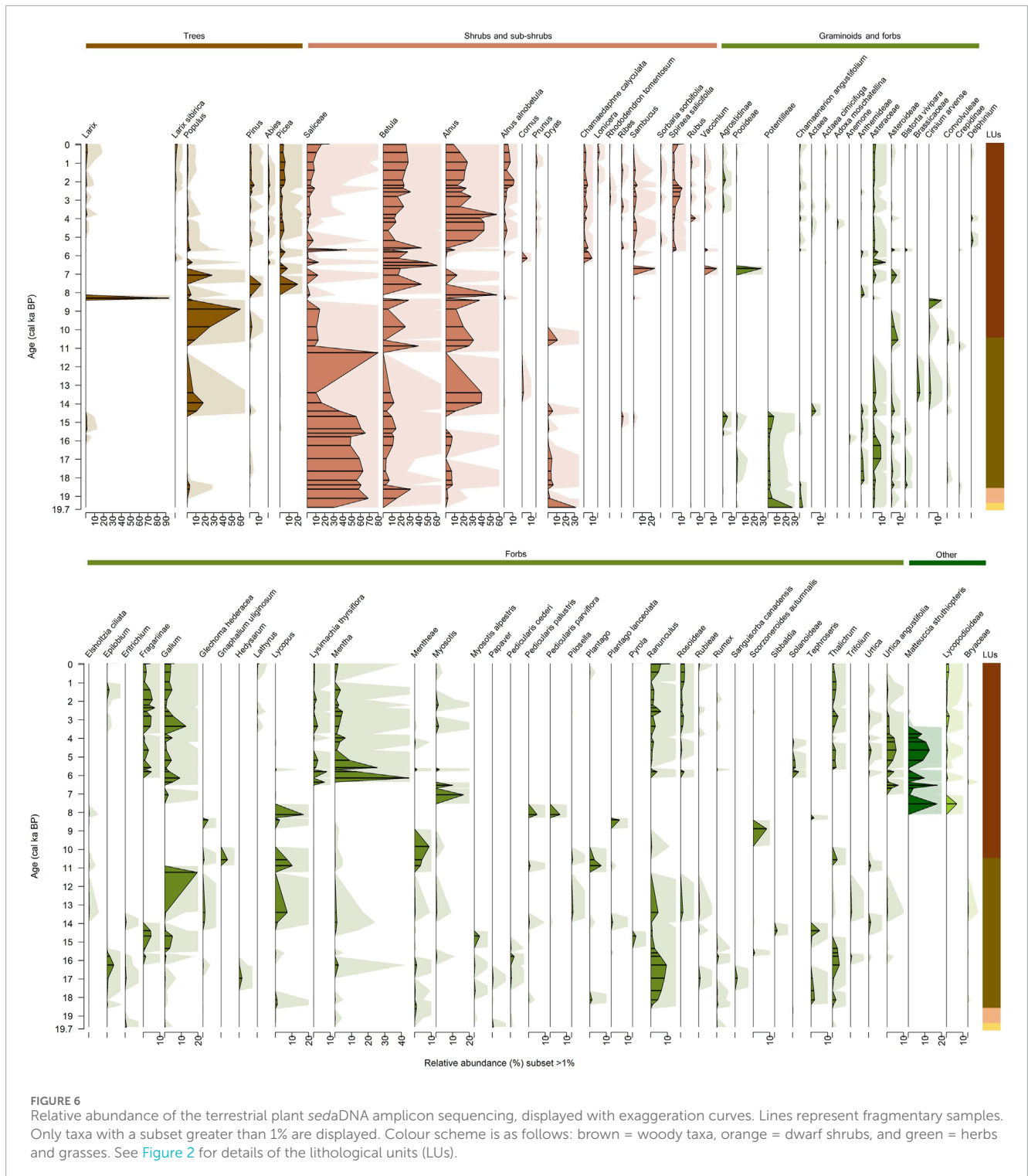
In LU4, between 9.8 cal ka BP and 1994 CE (885–6 cm), AP taxa become dominant (median 94%), while NAP constitute a median of 6%. The abundance of *Pinus* subg. *Diploxylon* and *P.* subg. *Haploxylon* significantly increase in LU4. Abundant AP taxa consist of *Picea* (median 25%), *Betula* sect. *Albae* (22%), *Pinus* subg. *Diploxylon* (20%), and *P.* subg. *Haploxylon* (10%). In LU3, *Larix* shows a marked peak at 8.9 cal ka BP (875 cm) with a maximum of 10.6% and *Picea* peaks at 6.5 cal ka BP (743 cm) with a maximum of 54.9%.

4.4.3 Non-pollen palynomorphs

In total, 29 non-pollen palynomorphs (NPPs) and two pollen of aquatic taxa were identified from 48 samples (Figure 8). NPPs in LU1 at 19.6 cal ka BP (1076 cm) constituted 14% of the assemblage (in relation to pollen sum), mainly of spores of *Encalypta* (4.3%), the fungus *Glomus* (4.3%), and the alga *Botryococcus* (3.7%).

In LU2, between 19.1 and 18.6 cal ka BP (1066–1058 cm), NPP abundance prominently increases, constituting a median of 53%. The composition of the NPPs is fungi (45%), such as *Sordaria* with a maximum of 40.3% and *Glomus* with a maximum of 19%. First invertebrate remains of *Macrobiotus* occur in LU2, but at a low abundance (<0.5%).

In LU3, between 17.1 and 10.4 cal ka BP (1051–894 cm), the abundance of NPPs is still high, constituting a median of 44%. NPP composition is mainly algae (31%) such as *Pediastrum* at up to 72%.



Spores of *Equisetum*, most likely *E. fluviatile*, are more abundant in this LU (median 3%). The share of fungi decreases, with *Glomus* up to 9% and *Sordaria* up to 2% only. Pollen of aquatic taxa *Nuphar* and *Potamogeton* occur in LU3, but at low abundance (less than 1% in total).

In LU4, between 9.8 cal ka BP and 1994 CE (885–6 cm), median abundance of NPPs decreases to 8%. NPPs of LU4 mainly consist of the alga *Pediastrum*, up to 47%. Other NPPs are less prominent.

4.5 Relationships of aquatic and terrestrial ecosystems with sedimentological and geochemical data

The first and second principal component (PC) axes of the aquatic ecosystem dataset explain 30.5% and 23.5% of the variance, respectively ([Figure 9A](#)) and the first and second PC axes of the terrestrial ecosystem dataset explain 33.4% and 14.7% of

the variance, respectively (Figure 9B). The differentiation within the environmental proxies are displayed by the biplots along PC1. XRF-derived Br is associated with TOC along the negative axis of PC1 in the aquatic dataset and along the positive axis of PC1 in the terrestrial ecosystem dataset, likely constituting the “organic” variables. High TOC and XRF-derived Br shows association with samples from the Mid-Holocene. XRF-derived Zr is mainly associated with samples from the Late Glacial along the positive axis of PC1. Samples from the Mid and Late Holocene are separated along PC1 of the aquatic ecosystem but are clustered along the negative axis of PC1 in the terrestrial ecosystem.

5 Discussion

5.1 Lake Khamra ecosystem development

5.1.1 Initial lake conditions

Overall, our results suggest that the coarse-grain deposits in the basal sections of LU1 to LU2 (19.6–18.4 cal ka BP, 1076–1052 cm) in the Khamra depression reflect fluvial activity, such as in a floodplain. Zr can be indicative of soil and heavy mineral loads from weathered rocks within the catchment (Rosenbaum et al., 1996) as it is signalling detrital input (Biskaborn et al., 2021b). Therefore, high XRF-derived Zr at the bottom of the core (Figure 3B) suggests high transport energy in the sedimentary sequence. The sequences of black gyttja layers in LU2 might have originated from sedimentation in a temporal pond-like water body in a boggy wetland. These layers align with a small TOC peak (9.4 wt%) at ca. 18.6 cal ka BP (Figure 3C) indicating productivity within the ephemeral pond. Inferred terrestrial plant communities support this finding, with *sedaDNA*-derived and microscopically identified spores of aquatic *Equisetum* indicating wetland (Zimmermann et al., 2017b; Bjune et al., 2022). *Equisetum* is characteristic of peatland and marshes (Hudson et al., 2023). Similarly, the green alga *Botryococcus* found in LU1 to LU2 is common in ephemeral ponds and peat bogs (Guy-Ohlson, 1992). The high prevalence of *sedaDNA* from aquatic plants like *Potamogeton*, *C. demersum*, and *Myriophyllum* further supports a wetland habitat, as these species are known to tolerate such environments (Lougheed et al., 2001). Finally, *sedaDNA*-derived diatom results (Figure 4) show that no diatoms were found in the oldest sample, which could be related to poor preservation and/or low aquatic productivity.

5.1.2 Lake development in the Late Glacial

Establishment of a lacustrine environment started at 18.4 cal ka BP as suggested by the change in the core lithology between LU2 and LU3 (Figure 3G) and occurrence of submerged and floating macrophytes (Figure 5) as well NPPs of algae and wet habitat-related spores (Figure 8). Lake Khamra sediments dated to 18.6–18.4 cal ka BP align with the post-LGM period. *SedaDNA*-derived indications of submerged *Potamogeton*, *Stuckenia* and *S. pectinata* from 18.4 cal ka BP corroborate the existence of a lacustrine environment. We infer that the lake was rather shallow as indicated by *sedaDNA* of floating *Nuphar lutea* and pollen grains of *Nuphar* occurring in the lake at 18.4 cal ka BP (Figure 8). Green algae colonies of *Pediastrum* are known as indicators of a shallow-water environment (Andreev et al., 2002; Kienast et al., 2005) and are

abundant from 18.4 cal ka BP. The occurrence of *sedaDNA*-derived submerged-emergent *Hippuris* at 18.4 cal ka BP supports this finding since *Hippuris* occurs in water bodies not deeper than 1 m (Mariash et al., 2018).

The diatom composition at ca. 17 cal ka BP displays a similar taxonomic composition to that of Lake Kotokel, to the east of Lake Baikal (Bezrukova et al., 2010) between 46 and 34 cal ka BP, which consists of pioneering small fragilarioids suggesting initial lake development. This diatom assemblage is also typical of initial stages of permafrost-thaw lakes (alaas lakes) in Central Yakutia (Pestryakova et al., 2012; Pestryakova et al., 2018; Baisheva et al., 2023) or shallow tundra thermokarst lakes in northern Yakutia (Biskaborn et al., 2012; Biskaborn et al., 2013b; Stoof-Leichsenring et al., 2015; Huang et al., 2020). Only epiphytic diatoms can survive during summer when shallow lakes evaporate and suffer from algal blooms and during long winters when shallow lakes are filled with ice (Biskaborn et al., 2012; Pestryakova et al., 2012; Pestryakova et al., 2018; Baisheva et al., 2024).

The lake was probably shallow until 14.7 cal ka BP, and likely did not have an outflow, as only the epiphytic diatom *P. elliptica*, typical of shallow lakes (Pestryakova et al., 2018), is abundant from 17 cal ka BP until 14.7 cal ka BP, suggesting low water clarity and high mineralisation. Productivity at this time was low, as shown by low TOC and Br (Figures 3C, D). In general, small fragilaroids in combination with low TOC are indicative of a cold lake environment (Biskaborn et al., 2012). It is likely that “*Staurosirella* sp.1 LKM-2011” found in Lake Khamra is *S. pinnata*. This species was found in Lake Satagay and indicated the initial shallow stage at ca. 10.3 cal ka BP (Baisheva et al., 2023). However, the ability of *Staurosira* lineages to adapt to various environmental conditions may lead to evolutionary divergence (Stoof-Leichsenring et al., 2015) thus complicating the species genetic indication (Stoof-Leichsenring et al., 2014). Small fragilaroids like *P. elliptica*, *Staurosirella*, and *S. pinnata* are pioneers because these species tolerate the cold climate conditions and can colonise benthic habitats during ice-covered periods (Biskaborn et al., 2012). *Staurosirella pinnata* has been described as typical of northern forest lakes (Pestryakova et al., 2018). The optimum pH for *Pseudostaurosira* and *Staurosirella* taxa found in Yakutian lakes ranges between 6.95 neutral to 7.91 alkaline, and conductivity ranges from 67 to 285 $\mu\text{S cm}^{-1}$, suggesting a preference for relatively low to moderate ion concentrations (based on Pestryakova et al., 2018).

We assume that the warming during the Bølling-Allerød led to the noticeable lake-ecosystem change at around 14.7 cal ka BP, shown by drastic changes in the Mn/Fe ratio and sedimentation rate. It is likely that a large lake body formed, with an increased water level, resulting in the occurrence of planktonic *Aulacoseira* at 14.7 cal ka BP, along with abundant *Staurosira* (Figure 4). The *Aulacoseira* genera pH optimum, typical in Yakutian lakes, ranges between 6.91 and 8.23 (Pestryakova et al., 2018). Climate warming in the Bølling-Allerød is evidenced by the presence of *C. hermaphroditica* from 14.5 cal ka BP to 13 cal ka BP, a species found where mean summer temperature is higher than 12°C (Kienast et al., 2005). Gradually, productivity starts to increase in the Bølling-Allerød, as shown by TOC and Br, resulting in an elevated sedimentation rate (Figures 3A, C, D). The gradual increase of the submerged macrophytes *P. perfoliatus* and *P. praelongus* support a lake water level rise from

14.4 cal ka BP. *Hippuris* declines, probably because of extensive interspecific competition caused by climate amelioration. Typically, *Hippuris* occurs in colder environments and is found in high-latitude and high-elevation lakes (Stoof-Leichsenring et al., 2022). A significant decline in macrophytes, which are generally warmth-indicators (Stoof-Leichsenring et al., 2022), especially *Callitriche hermaphroditica* (Kienast et al., 2005), is seen around 12.8 cal ka BP (Figure 5). The source of organic matter in the Bølling-Allerød shows a prevalence of terrestrial signals, with a TOC/TN_{atomic} ratio of 13.1 (Figure 3F).

5.1.3 Lake history in the Holocene

In the Early Holocene, after 11.2 cal ka BP, lake bioproductivity significantly increases, as reflected by higher TOC and Br (Figures 3C, D). Decreasing values of XRF-derived Zr after 11.2 cal ka BP (Figure 3B) indicate reduced erosion due to a denser vegetation cover and also partly explain increasing TOC and Br since 11.2 cal ka BP. A lithological change occurs in the Early Holocene at 10.5 cal ka BP (Figure 2B). The diatom composition shifts from epiphyton dominated to plankton dominated, as shown by *Aulacoseira* abundance (Figure 4) suggesting an increase in lake water level. Primary productivity inferred from a more aquatic TOC/TN_{atomic} ratio (10.4) can also reflect aquatic changes (Herzschuh et al., 2005). Biskaborn et al. (2012) suggest that the combination of a gradual decrease of TOC/TN_{atomic} along with an increase of planktonic *Aulacoseira* could imply a lake water-level increase, which is visible in Lake Khamra at 11.2 cal ka BP.

The pronounced decrease of planktonic diatoms from 8.2 cal ka BP until 6.5 cal ka BP, in the Mid-Holocene, could be explained by a decrease in lake water level. The prevalence of epiphytic taxa probably signals colonisation of a newly expanded lake periphery and is supported by the occurrence of benthic diatoms (Figure 4). The occurrence of epiphytic and benthic assemblages in the lake and an increase in the sedimentation rate (Figure 3A) reflect high bioproductivity. The highest peak of bioproductivity occurs between 8.2 cal ka BP and 6 cal ka BP, as shown by the TOC and Br peak (Figures 3C, D) along with the high association of the Mid-Holocene samples with TOC and Br in the PCA (Figure 9A). Newly occurring taxa are not abundant but do indicate warming, for example, the optimum water temperature is higher than 17°C for *Fragilaria construens*, *A. granulata*, and *Stephanodiscus* (Pestryakova et al., 2018). *Stephanodiscus* and *F. construens* prefer alkaline waters (based on Stenina, 2009, for example, *Stephanodiscus hantzschii* has a pH optimum of 8.74 and for *S. minutulus* it is 8.55 (Pestryakova et al., 2018)) and they usually occur in highly mineralised waters (Pestryakova et al., 2012).

A colder climate is inferred after ca. 4.5 cal ka BP, in the Late Holocene, as shown by the decline of warm-water preferring taxa such as *F. construens*, and later at ca. 2 cal ka BP, *A. granulata* and *Stephanodiscus* (Pestryakova et al., 2018). Arctic-alpine diatom species dominate, for example, *T. flocculosa*, *Aulacoseira subarctica*, and *A. valida* which are adapted to cold conditions (based on Stenina, 2009). *Tabellaria flocculosa*, which is typically abundant in tundra-forest sites (Pestryakova et al., 2018; Huang et al., 2020), indicates oligotrophic conditions (Stenina, 2009) in Lake Khamra during the Late Holocene.

5.2 Terrestrial ecosystem reconstruction

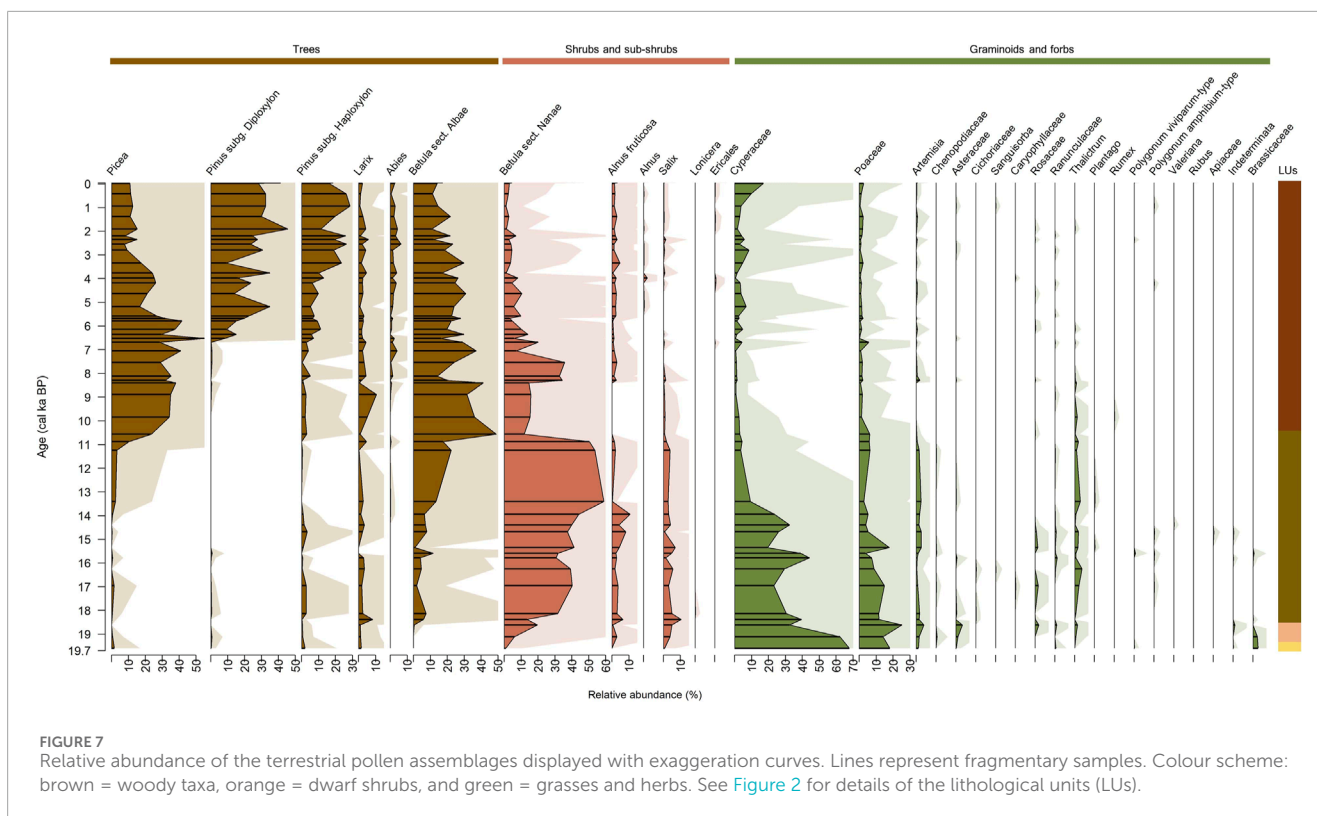
5.2.1 Wet tundra and herbivores in the post-LGM

Terrestrial vegetation in the Late Glacial from 19.6 cal ka BP to 18.4 cal ka BP was dominated by graminoids and forbs, particularly Cyperaceae and Poaceae with a few stands of *Larix* (larch), *Picea* (spruce), and other Pinaceae. Low pollen counts of underrepresented trees might hint at refugia during the Late Glacial, specifically for *Larix* rather than *Picea* and *Pinus* (Herzschuh, 2020). This finding is supported by other records along the Lena River in Upper Lena (Kobe et al., 2022b), Central Yakutia (Schulte et al., 2022a; 2022b), and west of the Verkhoyansk Mountain Range (Müller et al., 2010).

The PCA results show that the Late Glacial tundra taxa are strongly associated with XRF-derived Zr (Figure 9B). Low vegetation cover likely permitted high soil disturbance and the associated erosion subsequently increased sedimentation into the lake basin, as confirmed by high values of *Glomus*, which grows on disturbed soils (Del Val et al., 1999). Abundant coprophilous fungi, mainly *Sordaria* and *Sporormiella* (Figure 7), indirectly reflect the presence of numerous herbivores in the area and can be used as an indicator of large herbivores in Siberia (Andreev et al., 2011; Herzschuh et al., 2016). Palynological analysis (dated back to 50 cal ka BP) from Batagay also report abundant *Sordaria* NPPs and *sedaDNA* shotgun analyses have revealed a diverse mammalian community including mammoths, horses, and ruminants (Courtin et al., 2022). So far only Pleistocene bison remains have been found in the Lensky district (Boeskorov, 2004), close to Lake Khamra. Sparse terrestrial vegetation composition and catchment conditions around Lake Khamra were likely suitable for megaherbivores, as suggested by NPP results of coprophilous fungi (Figure 8). In the Late Glacial, wet tundra provided the food source for large grazing mammals (Axmanová et al., 2020). Hence potential prey animals in the area may explain why humans settled in the Lake Khamra region during the Upper Palaeolithic (35–10.5 ka BP) southwest of Lake Khamra (Boeskorov, 2004).

5.2.2 Shrub tundra (18.4 cal ka BP–14.5 cal ka BP)

Pollen data document the expansion of *Salix*, *Betula* sect. *Nanae*, *Pinus pumila*, *A. fruticosa*, and *Larix* trees in the vicinity of Lake Khamra since 18.4 cal ka BP. The vegetation cover after 18.4 cal ka BP consisted of shrub tundra taxa such as *Betula nana* (dwarf-birch) and *Salix* (willow). Our data suggest climate amelioration after the LGM, with the terrestrial vegetation composition (Figures 6,7,) signalling moist habitats around Lake Khamra. A dense shrub layer of *Betula* sect. *Nanae*, *Pinus* subg. *Haploxylon*, and *A. fruticosa* (dwarf birches, pine, and shrubby alders) around the lake indicates a warming climate (as described in Andreev et al., 2002; 2004; 2011). *Pinus* subg. *Haploxylon* pollen is difficult to differentiate (Andreev et al., 2022) because it could be the shrub *P. pumila* (dwarf stone pine; Lozhkin et al., 2007) or the tree species, for example, *P. sibirica* (Andreev et al., 2014), or both (Müller et al., 2010). However, *Pinus* subg. *Haploxylon* -type in the Late Glacial is usually inferred to be the shrub *P. pumila* which can better tolerate the cold and dry climate of this time (Andreev et al., 2022) suitable for this time and not the tree species *P. sibirica* or *P. sylvestris* (Scots pine). Similar reconstructions of climate amelioration from 18 cal ka BP to 14 cal ka BP have been drawn from the Lake Ilirney record in Chukotka,



shown by the increase of dwarf shrubs like *A. fruticosa* with *Betula nana* and shrubs of Salicaceae (Andreev et al., 2021; Huang et al., 2021).

A decreased prevalence of herbivores (Stuart, 1999; Plasteeva et al., 2020) is captured by the prominent decrease of fungal spores related to herbivores in the NPP spectra of Lake Khamra from ca. 18.4 cal ka BP (Figure 8). The rapid increase of *Betula* at 18 cal ka BP could suggest the northward movement of megafauna (Stuart, 1999) or even the extinction of some species (Monteath et al., 2021). The diet of mega-herbivores included not only graminoids and forbs, which likely benefitted from trampling (Willerslev et al., 2014), but also *Betula* along with other shrubs (Axmanová et al., 2020) and thus an absence of megaherbivores could lead to an increase in the size and abundance of trees (Doughty et al., 2010).

5.2.3 Bølling-Allerød broadleaf woodland and Younger Dryas tundra

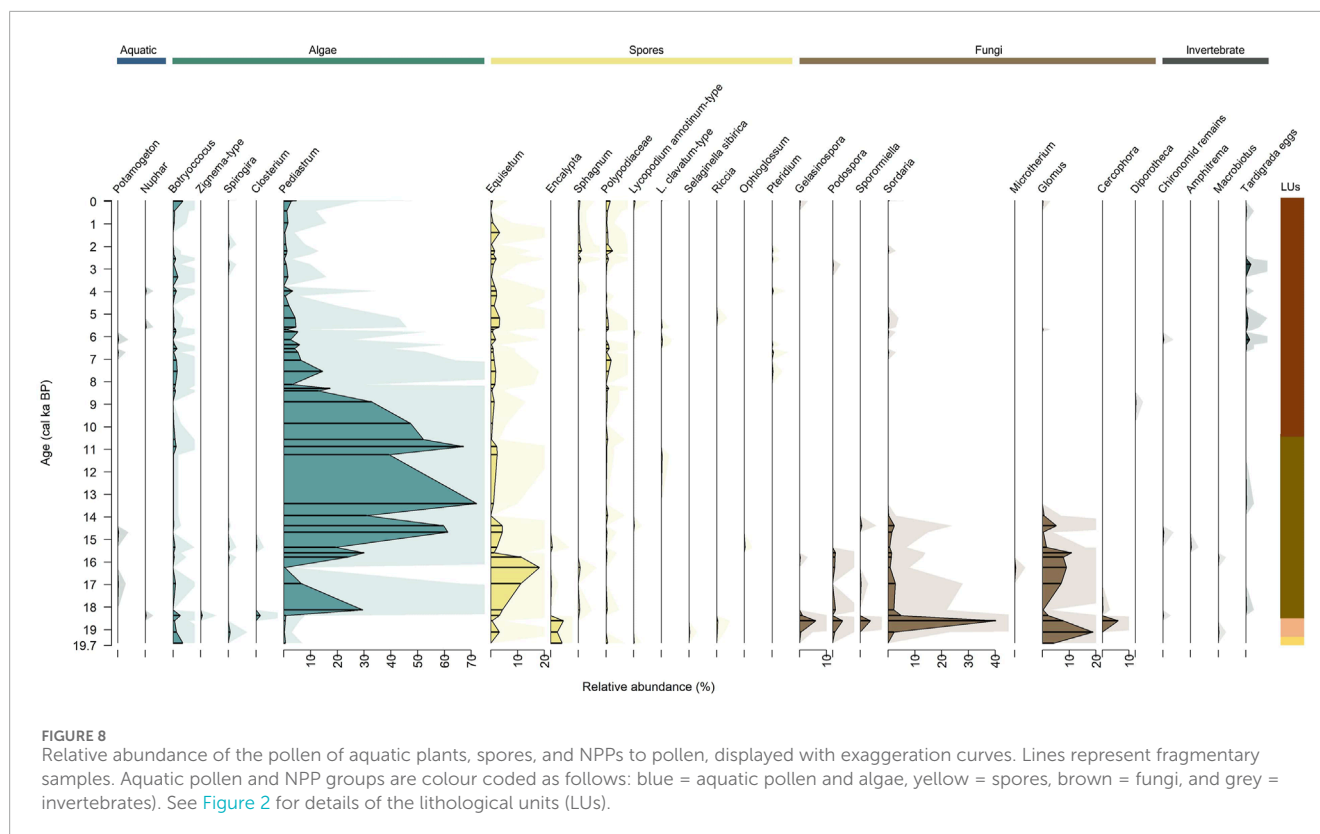
The warming at 14.7 cal ka BP led to broadleaf woodland development, composed mainly of *P. tremula* (aspen, *sedaDNA*), and *Betula* sect. *Albae* (pollen). Tundra plants decreased according to the *sedaDNA* (Figure 6) and there is some occurrence of other tree taxa such as *Picea*, *Pinus*, and *Larix* alongside shrubs of *Salix*, *Betula*, and *Alnus* at low counts. *SedaDNA*, which is considered more of a local signal (Jørgensen et al., 2012; Liu et al., 2020), shows *Larix* and *Picea* from 14.7 cal ka BP (Figure 6). The pollen record, which captures a signal from the wider regional area compared to the *sedaDNA*, shows the presence of *Larix* refugia already before the Bølling-Allerød (Figure 7). *SedaDNA* results capture a higher taxonomic level than the pollen data,

especially after matching amplicon sequencing results against the customised database for Siberian plants (Courtin et al., in review), thus limiting the likelihood of erroneous identifications. The samples from the Late Glacial and the Bølling-Allerød interstadial cluster together in the PCA, suggesting similar climatic conditions (Figure 9B).

We see Younger Dryas cooling in the Lake Khamra region by a decrease in the woody taxa such as *P. tremula*, *Betula*, and *Alnus* from ca. 13.4 cal ka BP and *Salix* until the Early Holocene (Figures 6,7), indicating shrubby tundra. Younger Dryas cooling at ca. 12.7 to 11.7 cal ka BP was synchronous across eastern Siberian sites, being reported as explicitly cold and dry from the Verkhoyansk Mountain Range sites (Werner et al., 2010; Andreev et al., 2022) and from Lake Kotokel in the eastern Baikal region (Bezrukova et al., 2010; Kobe et al., 2022a). Vegetation during this cold stage was typically shrubby and herbaceous tundra as reconstructed from Lake Kotokel (Tarasov et al., 2009), Dyanushka peat (Werner et al., 2010), and Lake Emanda between ca. 12.9 and 11.6 cal ka BP (Andreev et al., 2022). Our results align well with regional signals reported from southern and Central Yakutia by Andreev et al. (1997) that show a decline in tree taxa and an increase of graminoids and forbs.

5.2.4 Taiga in the Early Holocene

Taiga forest establishment is noticeable from the re-establishment of broadleaf tree taxa *P. tremula* and *Betula* sect. *Albae*, and the establishment of needleleaf tree taxa *Picea* and *Larix* by 11.2 cal ka BP. Forest establishment is also shown by the reduction of *sedaDNA*-derived and pollen-derived *Salix*, Cyperaceae, and Poaceae. A succession of sensitive arctic-alpine vegetation to woody plant communities occurs with



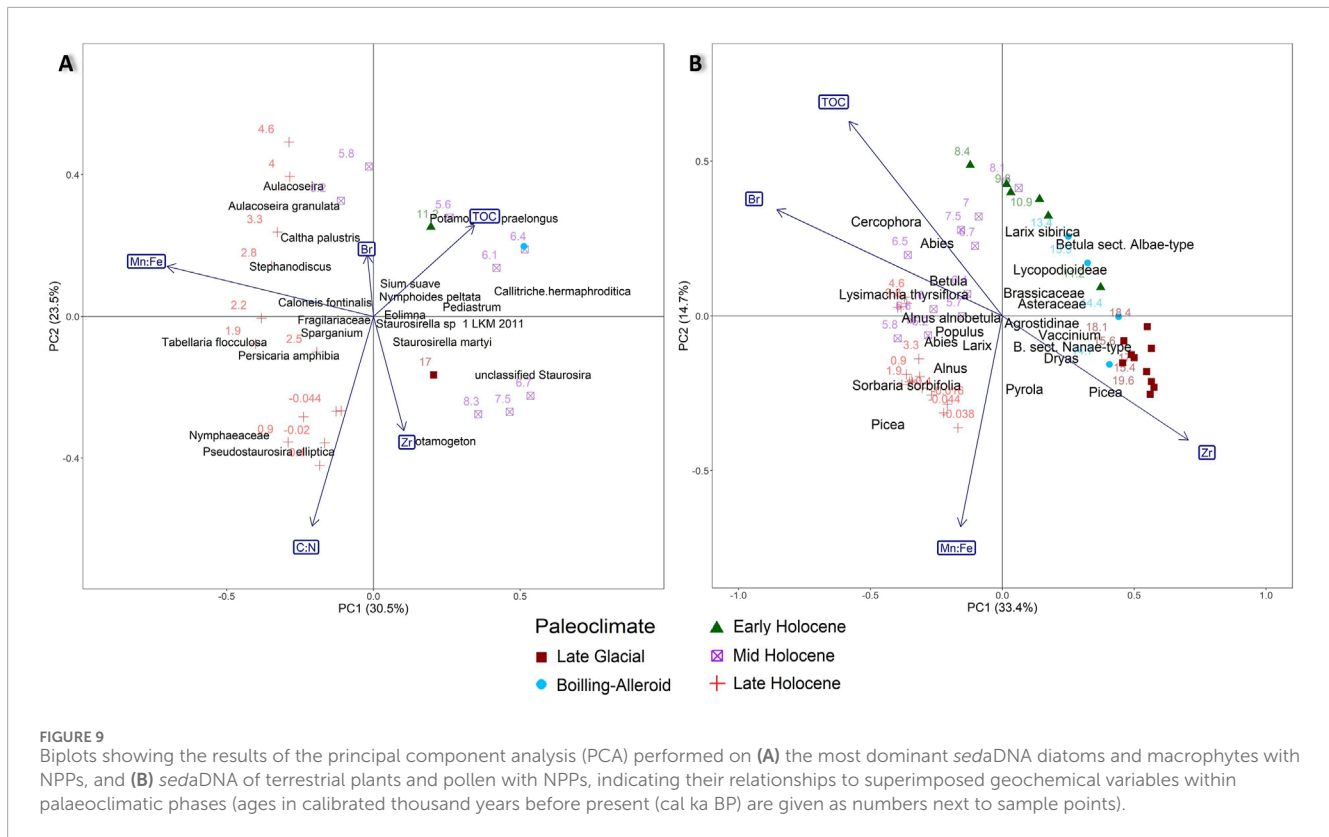
climate warming (Pearson et al., 2013; Hagedorn et al., 2014; Brodie et al., 2019), which is seen in the vegetation history record of Lake Khamra (Figures 6,7).

We observe a decrease in the *sedaDNA* of *Dryas* at ca. 10 cal ka BP and an increase in *Larix* pollen at ca. 9.5 cal ka BP. These changes can be indicative of the transition from tundra to taiga (as in Niemeyer et al., 2015; Li et al., 2021). *Larix* is generally known to be underrepresented in pollen records due to its relatively low pollen production, dispersal, and preservation in sediments (Edwards et al., 2000; Brubaker et al., 2005; Schulte et al., 2022b). The peak of *Larix* was recorded by pollen at 8.9 cal ka BP and by *sedaDNA* slightly later at 8.5 cal ka BP. *Populus tremula* became established around Lake Khamra by 9.5 cal ka BP (Figure 6). *Populus tremula* is a common succession species, and often forms in a post-fire forest with sufficient moisture availability (Troeva et al., 2010). Wildfire occurrence was found to be highly probable in Central Yakutia during the Early Holocene (Katamura et al., 2006; 2009), coinciding with increased abundance of *Populus* at Lake Satagay (Glückler et al., 2022). However, at Lake Khamra *P. tremula* and the disturbance indicator *Chamaenerion angustifolium* (fireweed) do not occur at the same time. Analysis of *sedaDNA* made it possible to detect *P. tremula* forest establishment around Lake Khamra by 9.5 cal ka BP, and in Lake Bolshoe Toko, Western Beringia, it was present since the Early Holocene from 11.5 cal ka BP to 5 cal ka BP (Courtin et al., 2021). In contrast, *Populus* is absent in the vegetation reconstructions based only on palynological analyses from the Lake Baikal region. Brubaker et al. (2005) noted that it is difficult to identify pollen of *Populus*, because of poor preservation in lake sediments.

5.2.5 Mixed taiga in the Mid and Late Holocene

Mixed forest establishment, starting at 6.5 cal ka BP and dominated by evergreen *Picea*, *Pinus* subg. *Diploxylon* (*P. sylvestris*, Scots pine), and summergreen *Betula* and *Larix*, can be deduced from the pollen data (Figure 7). *Picea* is abundant in the pollen several millennia earlier, but is underrepresented in *sedaDNA*, showing a time lag before occurring in the vicinity of the lake. *Abies sibirica*, an indicator species for taiga (Müller et al., 2010), is present since the Bølling-Allerød but better represented in the catchment after 8.5 cal ka BP according to the pollen data (Figure 7) and in the lake vicinity after 6.5 cal ka BP according to *sedaDNA* (Figure 6). *Pinus sylvestris* could establish on the sandy soils in the lake vicinity (Glückler et al., 2022). *Abies sibirica* (Siberian fir) and *L. sibirica* (Siberian larch) occur in the *sedaDNA* record at the end of the Mid-Holocene (at 6.3 cal ka BP) and are indicative of permafrost retreat and may reflect isolated permafrost (Tchebakova et al., 2009), as well as low winter temperatures and lower precipitation (Pelánková et al., 2008).

It is evident that *M. struthiopteris* was present not only in the Early Holocene at 10.5 cal ka BP, but became abundant in the Mid-Holocene *sedaDNA* record between 7.5 and ca. 3.6 cal ka BP (Figure 6), supporting the inference of a warm period. This fern taxon typically occurs in the boreal region, thrives in environments with mild winters, minimal frost, and warm summers with high availability of water (Odland, 1992). Modern vegetation without *M. struthiopteris* around Lake Khamra developed around 3.6 cal ka BP. A fire study and high-resolution pollen investigation covering the last 2300 years at Lake Khamra (Glückler et al., 2021) shows that short-term occurrences of evergreen trees and sedges overlap with active biomass burning, but finds no evidence



for prominent shifts in the vegetation development for the last two millennia. Palaeofire reconstructions going further back in time would be beneficial to enhance our understanding of the drivers causing environmental changes and catchment vegetation dynamics.

5.3 Interaction between the aquatic and terrestrial ecosystems in relation to climate change in eastern Siberia

Modern Lake Khamra fills a depression in an intermontane basin (Glückler et al., 2021) in an area that was non-glaciated area during the Glacial (Margold et al., 2016). When the Lake Khamra record began, the inferred wet-tundra environment suggests a sufficient water supply for lake development via precipitation and snow melt in the deepest part of the basin, from where the core was taken (Figure 1B). But the contribution of meltwater from thermokarst degradation in the lake's catchment cannot be excluded, as during the LGM the area was underlain by continuous permafrost (Shahgedanova, 2002). Although today the area lies within the sporadic permafrost zone (Obu et al., 2019), no features of active permafrost degradation have been observed in the close vicinity of the lake (Glückler et al., 2021). Increased water supply along with low vegetation cover, as evidenced by *sed*aDNA and pollen of terrestrial plants and XRF-derived Zr, allowed ephemeral ponds to form during the summer, which later developed into a lake. Thus, we assume that higher Zr in the Late Glacial sediments could indicate strong erosion unhampered by the sparse vegetation.

The Lake Khamra sediment record (Table 2) in the glacial-interglacial transition after the LGM signals a wet-tundra environment between 19.6 and 18 cal ka BP. Willerslev et al. (2014) report the transition from dry-steppe tundra to wet-tundra after the LGM in the circum-Arctic region. Similar climate fluctuations have been inferred from environmental records from the trans-Baikal region and central and northern Yakutia where wet-tundra became established from 19 to 17 cal ka BP (Binney et al., 2017). After the wet-tundra development, the Lake Khamra record shows an expansion of shrubs and the development of a shrub-tundra landscape in the Late Glacial. Similarly, the Lake Kotokel record, located to the east of Lake Baikal, shows a gradual increase in pollen of dwarf shrubs *P. pumila*, *A. fruticosa*, *Betula* sect. *Nanae*, *B. sect. Albae* (tree birch), and *Salix* after 18.5 cal ka BP (Bezrukova et al., 2010). Low counts of tree taxa and high abundance of shrubs could indicate glacial refugia in the Lake Khamra region for shrubs along with tree taxa.

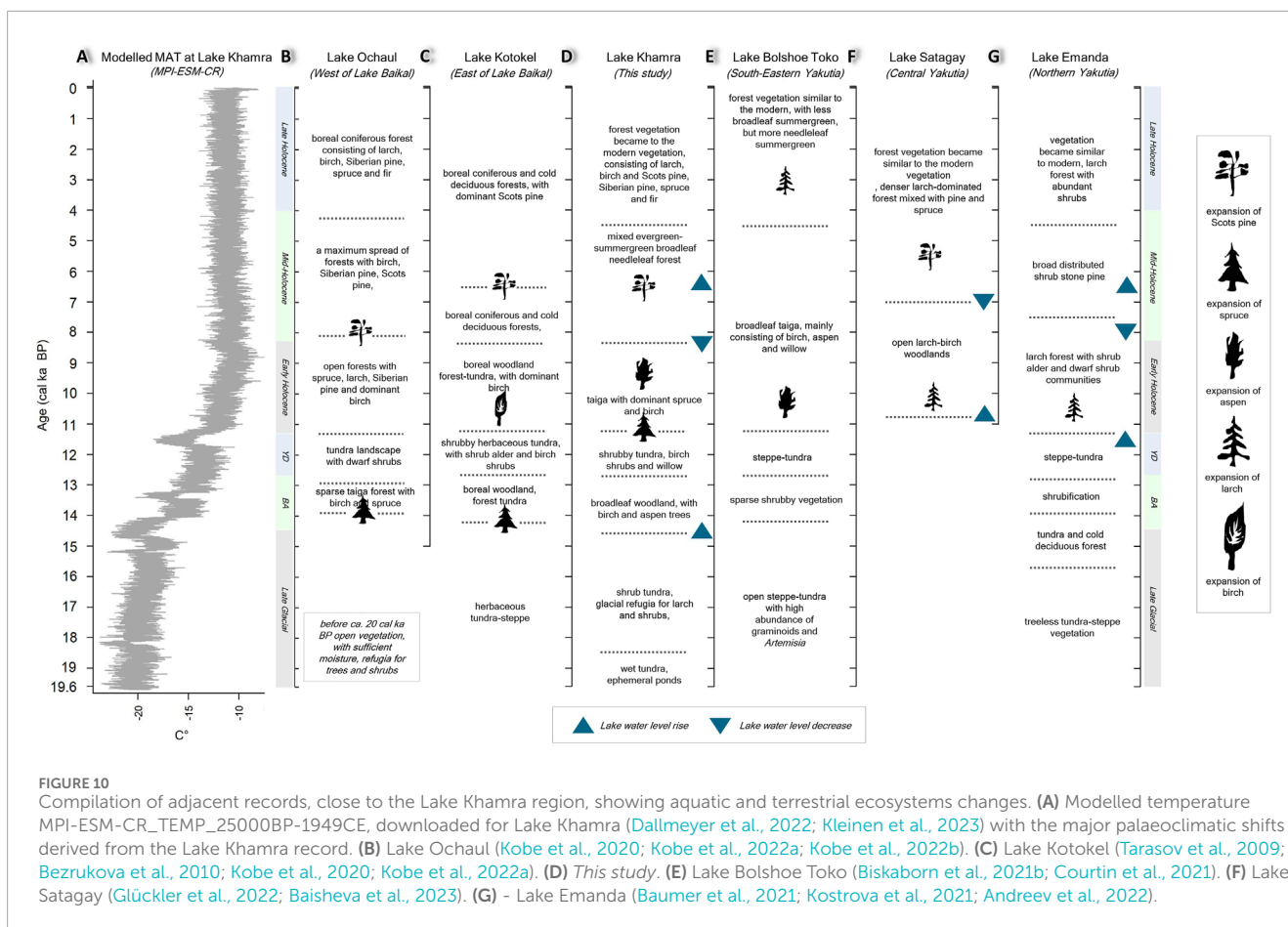
Progressive warming during the Bölling-Allerød between 14.5 and 12.7 cal ka BP (Figure 10A) has its impact on both the aquatic and terrestrial ecosystems. The growing terrestrial vegetation cover in the Khamra region decreased sediment transport into the lake as indicated by a gradual decline of Zr (Figure 3B). The climate amelioration caused the lake water level rise indicated by planktonic diatoms *sed*aDNA (Figure 10D). The occurrence of the emergent macrophyte *Callitriche hermaphroditica* and the submerged *Stuckenia pectinata* suggest warm summer temperatures. The results from *sed*aDNA and pollen data show the development of broadleaf forest around Lake Khamra. Warmer climate and higher

TABLE 2 Summary of the palaeoenvironmental reconstruction and proxies used for the aquatic and terrestrial ecosystems from Lake Khamra ordered by lithological unit [LU]. Each LU from sedimentary core EN20001 is given with its depth and modelled ages.

Aquatic ecosystem		LU	Terrestrial ecosystem	
Reconstruction	Proxies		Reconstruction	Proxies
Late Glacial (19.6–14.5 cal ka BP)				
Cold organic-poor ephemeral ponds with organic-rich gyttja layers in an ephemeral pond	XRF-derived Zr, coarse grain lithology, NPP, small peak of TOC	[LU1] 1076–1067 cm 19.6 to 19.1 cal ka BP	Wet tundra Sparse vegetation cover with abundant graminoids and forbs, herbivores, likely megafauna, refugia of <i>Larix</i>	Pollen, NPP, sedaDNA terrestrial plants, XRF-derived Zr
		[LU2] 1067–1052 cm 19.1 to 18.4 cal ka BP		
Shallow lake with moderate bioproductivity, indicative epiphytic diatoms, macrophytes and NPPs of algae	TOC; XRF-derived Br; sedaDNA diatoms, macrophytes, NPPs	[LU3] 1052–892 cm 18.4 to 10.5 cal ka BP	Shrub-tundra biome Refugia of shrubs	SedaDNA terrestrial plants, pollen
Bølling-Allerød (14.5–12.7 cal ka BP)				
Large lake body Occurrence of planktonic diatoms	SedaDNA diatoms and macrophytes; NPP		Broadleaf woodland establishment Decrease of tundra biome plants in the lake's vicinity, likely megafauna extinction	SedaDNA terrestrial plants, pollen, XRF-derived Zr
Younger Dryas (12.7–11.2 cal ka BP)				
Lake water cooling Decrease of warm water and summer temperature preferring taxa	SedaDNA diatoms and macrophytes; NPP		Shrubby tundra Decrease of tree taxa	SedaDNA terrestrial plants, pollen, TOC, XRF-derived Br
Early Holocene (11.2–8.2 cal ka BP)				
Lake water-level rise from 11.2 cal ka BP shown by high abundance of planktonic <i>Aulacoseira</i>	SedaDNA diatoms and macrophytes; NPP	[LU4] 892–0 cm 10.5 cal ka BP to 2020 CE	Taiga establishment from 11.2 cal ka BP, <i>Picea</i> , <i>Betula</i> Populus forest establishment since 9.5 cal ka BP	SedaDNA terrestrial plants, pollen, TOC, XRF-derived Br
Mid-Holocene (8.2–4 cal ka BP)				
Lake level decrease from ca. 8.2 cal ka BP to 6.5 cal ka BP Lake expansion from 6 cal ka BP compositional turnover of diatoms towards planktonic and benthic	High TOC, sedaDNA diatoms and macrophytes; NPP		Mixed evergreen-summergreen forest establishment from 6.5 cal ka BP	SedaDNA terrestrial plants, pollen
Late Holocene (4 cal ka BP - modern)				
Cooling from 5 cal ka BP composition of diatoms and macrophytes composition shows cool water preferring taxa; moderate bioproductivity	SedaDNA diatoms and macrophytes, NPP; TOC, XRF-derived Br		Mixed evergreen-summergreen forest from 3.6 cal ka BP similar to modern	SedaDNA terrestrial plants, pollen

humidity around Lake Baikal after the LGM (15.8 cal ka BP) and during the Bølling-Allerød resulted in the development of open forests (Demske et al., 2005), as shown by the occurrence of tree sedaDNA including *Betula* sect. *Albae* and very low counts of *P. sylvestris* and *Larix* pollen. Tarasov et al. (2009), Tarasov et al. (2021) and Bezrukova et al. (2010) also describe warm and wet conditions for 13.5–12.7 cal ka BP that supported boreal woodland and forest-

tundra development with *Picea* and *Betula* sect. *Albae* in the Lake Kotokel record (Figure 10C), east of Lake Baikal. A pollen record from Lake Ochaul, west of Lake Baikal, documents *Betula* sect. *Albae* forest development with *Picea* from ca. 13.5–12.6 cal ka BP (Figure 10B), reflecting a warming climate and the existence of forest patches during the Bølling-Allerød (Kobe et al., 2020). Pollen studies from northern and eastern Yakutia indicate shrubification



around Lake Billyakh (Müller et al., 2010) and shrubification around Lake Emanda (Andreev et al., 2022) during the Bølling-Allerød (Figure 10G). The Bølling-Allerød warming is reflected as a south to north and west to east palaeoclimate transition showing woodland development with the evergreen needleleaf tree taxa in the Lake Baikal region to broadleaf woodland in the Lake Khamra region to shrub expansion, but no woodland in north-eastern Yakutia.

Lake Khamra's terrestrial ecosystem before the Holocene was represented by wet-tundra (19.6–18 cal ka BP), shrub tundra (18.4–14.5 cal ka BP), and broadleaf forest establishment (14.5–12.7 cal ka BP). These palaeobiomes are more in alignment with the records from the west Baikal region than records from northeastern Yakutia (Figures 10B, C).

Climate warming at the Late Glacial–Holocene transition in the Northern Hemisphere (Herzschuh et al., 2023) caused taiga forest establishment at around 11.2 cal ka BP with needleleaf *Picea* and *Larix* and broadleaf *P. tremula* and *Betula* sect. *Albae* in the Lake Khamra region. South-west of Lake Khamra, re-establishment of broadleaf woodland with dominant *Betula* sect. *Albae* started at 11.5 cal ka BP at Lake Kotokel and after 10.5 cal ka BP boreal coniferous and cold deciduous forests became fully established (Tarasov et al., 2009; Bezrukova et al., 2010; Tarasov et al., 2021). Taiga forest with dominant *Betula* sect. *Albae* and increasing values of coniferous taxa established at Lake Ochaul, west of Lake Baikal, by ca. 11.7 cal ka BP (Kobe et al.,

2020). North-east of the Khamra region, the Lake Satagay record (Glückler et al., 2022) shows open forest (Figure 10F), dominated by *Larix* and the Lake Emanda record also shows *Larix* forest (Andreev et al., 2022) in the Early Holocene (Figure 10G). The cold deciduous forest starts after 9.3 cal ka BP at Lake Billyakh (Müller et al., 2010). Establishment of deciduous needleleaf forests seen in records from northern and Central Yakutia from 9 cal ka BP (Binney et al., 2017) show a time lag compared with the Baikal region and Lake Khamra records. Taiga establishment with increasing evergreen needleleaf taxa to the west of the Lake Baikal and Khamra regions is similar (Figure 10), and could be indicative of permafrost retreat.

The warmer and wetter climate in the Early Holocene (11.2 cal ka BP) caused the lake water-level rise of Lake Khamra as shown by compositional turnover towards planktonic diatoms. Similar findings have been reported from the Verkhoyansk Mountain Range lakes, Lake Vorota and Lake Emanda, to the north-east of Lake Khamra, at ca. 11 cal ka BP where lake deepening was inferred from planktonic diatom dominance, mainly *Aulacoseira* (Firsova et al., 2021) and *Cyclotella* (Kostrova et al., 2021). These findings suggest increased precipitation, as supported by the diatom oxygen isotopic values which indicate an increase of meltwater at Lake Emanda (Kostrova et al., 2021). Kostrova et al. (2021) propose that weakening of the Siberian High weather system in the Early Holocene (Mackay, 2007) could contribute to the enhanced westerly moisture supply.

In the Mid-Holocene, at ca. 8.2 cal ka BP, the Lake Khamra vegetation record shows an increase of the shrubs *Betula* sect. *Nanae* and *A. fruticosa*. At the same time the diatom record shows the turnover of planktonic dominance to epiphytic-benthic taxa dominance, indicating a lake level decrease. The lake water level of Lake Khamra rises again around ca. 6.5 cal ka BP, indicated by planktonic diatoms abundance. Similar changes are reported from Lake Emanda, with the dominance of benthic diatoms between ca. 8 and 6.5 cal ka BP (Kostrova et al., 2021). At Lake Vorota, further to the east, similar changes happened a millennium earlier with a strong lake water level decrease at 9 cal ka BP and a strong lake water level rise at ca. 8.3 cal ka BP (Firsova et al., 2021).

The lake records along a south-west to north-east transect also show the evergreen tree taxa expansion in the Mid-Holocene. The establishment of evergreen-summergreen needleleaf mixed taiga forests is indicated by the occurrence of *P. sylvestris* from 6.5 cal ka BP in the Lake Khamra region. At Lake Ochaul, to the south-west of Lake Khamra, *P. sylvestris* expansion occurred at 8 cal ka BP (Kobe et al., 2022a) while at Lake Satagay, a site to the north-east of Lake Khamra, expansion started later at 5.5 cal ka BP (Glückler et al., 2022). At other Central Yakutian sites with a well-drained substrate, *P. sylvestris* established between six and 5.3 cal ka BP (Katamura et al., 2006; Katamura et al., 2009). Towards the northeast, the Lake Billyakh record indicates cold deciduous forest throughout the Holocene (Müller et al., 2010). An exception to the pattern is the record from Lake Kotokel, near to Lake Ochaul in the south-west, where *P. sylvestris* establishment was delayed until 6.7 cal ka BP.

In the Late Holocene, a colder climate is indicated in the Lake Khamra record by the abrupt decrease of warm-water preferring macrophytes and diatoms at ca. 4.5 cal ka BP. The cooling likely caused the distinct decline in macrophyte abundance, similar to the Younger Dryas cooling, for example, the decline in *S. pectinata* (= *Potamogeton pectinata*), which is known as a warm-water preferring species (Herzschuh et al., 2010). Cooling is also indicated by the abrupt decline of the fern *M. struthiopteris* at around 3.6 cal ka BP. Cooling in the Lake Baikal region detected by isotopic values of diatoms, is already apparent at 6 cal ka BP, and has been connected to the intensification of the Siberian High (Mackay, 2007). A comprehensive study on the hydroclimatic regime for the past 225 years, in a parallel short sediment core from Lake Khamra, reveals that the lake oxygen diatom record is mainly influenced by early winter precipitation, which correlates with a winter NAO index (Stieg et al., 2023). The lake is not currently affected by the evaporation, unlike the Central Yakutian lakes (Wetterich et al., 2008).

6 Conclusion

Our multiproxy approach to assessing the Lake Khamra palaeoenvironmental record covering the last 19.6 cal ka BP provides new insights into the long-term history of forest establishment, glacial refugia of trees and lake development in south-western Yakutia. Data from diatoms, aquatic and terrestrial plant *sedDNA*, pollen, and NPPs, in combination with

sedimentological and biogeochemical proxies including XRF-derived elements, TOC and the TOC/TN_{atomic} ratio demonstrate the complementarity of our chosen proxies for palaeoecological reconstruction and exemplify the value of reconstructing aquatic and terrestrial ecosystems together. Moreover, terrestrial and aquatic plants *sedDNA* amplicon sequencing matched against a customised Siberian plants database enhanced the reconstruction of both ecosystems by providing a more comprehensive and a higher taxonomic resolution of identification compared to the results of classic pollen analyses.

Macrophytes deduced from *sedDNA* combined with macrophytes and NPPs detected from pollen provide a comprehensive overview of the aquatic ecosystem evolution and its response to climate and fluctuations in lake water level. Our results suggest that lake development started in the Late Glacial at 18.4 cal ka BP. In the Bølling-Allerød and in the Early Holocene, lake water-level rise is indicated by the abundant planktonic diatoms and deep-water preferring submerged macrophytes. A short period of lake water-level decrease is indicated by dominant epiphytic diatoms in the Mid-Holocene between 8.2 and 6.5 cal ka BP.

Woodland development shaped the main catchment changes from the Late Glacial to the Bølling-Allerød around Lake Khamra, by reducing erosion. The vegetation changed from wet-tundra in the Late Glacial, through woodland expansion in the Bølling-Allerød and taiga forest establishment in the Early Holocene, to mixed evergreen-summergreen needleleaf-broadleaf forest establishment in the Mid-Holocene. The reconstructed palaeobiomes from the Lake Khamra record are more in alignment with the records from the west Baikal region than records from north-eastern Yakutia during the Late Glacial and the Early Holocene. For the Mid and Late Holocene we observe longer time lags for palaeobiome development compared to the palaeorecords north-east of Lake Khamra. The Lake Khamra record closes a gap in the transitional region between existing studies in the Lake Baikal region and Central Yakutia, providing data from an understudied area and helping to enhance our understanding of vegetation dynamics, and glacial refugia as well as lake development during the Glacial and the Holocene.

Data availability statement

The datasets presented in this study can be found in online repositories. The names of the repository/repositories and accession number(s) can be found in the article/Supplementary Material.

Author contributions

IB: Conceptualization, Data curation, Formal Analysis, Funding acquisition, Investigation, Methodology, Project administration, Validation, Visualization, Writing–original draft, Writing–review and editing. BB: Conceptualization, Data curation, Formal Analysis, Investigation, Methodology, Writing–review and editing. KS-L: Data curation, Formal Analysis, Investigation, Methodology, Writing–review and editing. AA: Data curation, Formal Analysis, Investigation, Methodology, Writing–review and editing. BH: Writing–original draft, Writing–review

and editing. SM: Investigation, Writing–review and editing. LU: Resources, Writing–review and editing. EZ: Resources, Writing–review and editing. RG: Visualisation, Writing–review and editing. ED: Writing–review and editing. LP: Conceptualization, Funding acquisition, Resources, Writing–review and editing. UH: Conceptualization, Data curation, Funding acquisition, Methodology, Project administration, Resources, Supervision, Writing–original draft, Writing–review and editing.

Funding

The author(s) declare financial support was received for the research, authorship, and/or publication of this article. Open Access funding enabled and organised by Projekt DEAL. This study was supported through the projects by ERC consolidator grant no. 772852 to UH (PI) and partially by FSRG-2023-0027. IB was supported by DAAD e.V. (DAAD: 91775743), a short-term grant from AWI Graduate School (POLMAR), and a PhD Completion Scholarship provided by University of Potsdam. RG was funded by AWI INSPIRES (International Science Program for Integrative Research in Earth Systems).

Acknowledgments

We would like to thank the organisers and expedition members from the Alfred Wegener Institute Helmholtz Centre for Polar and Marine Research (AWI) and the BIOM Laboratory of the Institute of Natural Sciences of the M.K. Ammosov North-Eastern Federal University (NEFU) of the pre-Covid expedition “Khamra-2020” in March 2020, especially Jan Kahl and Aleksey A. Pestryakov for their support. We also acknowledge the help of Barbara von Hippel and student workers Linda Siebert and Paula Kosel with

References

- Alsos, I. G., Lammers, Y., Yoccoz, N. G., Jørgensen, T., Sjögren, P., Gielly, L., et al. (2018). Plant DNA metabarcoding of lake sediments: how does it represent the contemporary vegetation. *PLoS ONE* 13, e0195403. doi:10.1371/journal.pone.0195403
- Alsos, I. G., Rijal, D. P., Ehrlich, D., Karger, D. N., Yoccoz, N. G., Heintzman, P. D., et al. (2022). Postglacial species arrival and diversity buildup of northern ecosystems took millennia. *Sci. Adv.* 8, eabo7434. doi:10.1126/sciadv.abo7434
- Alsos, I. G., Sjögren, P., Edwards, M. E., Landvik, J. Y., Gielly, L., Forwick, M., et al. (2016). Sedimentary ancient DNA from Lake Skartjørna, Svalbard: assessing the resilience of arctic flora to Holocene climate change. *Holocene* 26, 627–642. doi:10.1177/0959683615612563
- Andreev, A. A., Klimanov, V. A., and Sulerzhitsky, L. D. (1997). Younger Dryas pollen records from central and southern Yakutia. *Quat. Int.* 41 (42), 111–117. doi:10.1016/S1040-6182(96)00042-0
- Andreev, A. A., Klimanov, V. A., and Sulerzhitsky, L. D. (2002). Vegetation and climate history of central Yakutia during the Holocene and late Pleistocene. *Bot. Zhurnal* 87 (7), 86. (in Russian).
- Andreev, A. A., Nazarova, L. B., Lenz, M. M., Böhmer, T., Strykh, L., Wagner, B., et al. (2022). Late quaternary paleoenvironmental reconstructions from sediments of Lake Emanda (Verkhoyansk mountains, east Siberia). *J. Quat. Sci.* 37, 884–899. doi:10.1002/jqs.3419
- Andreev, A. A., Raschke, E., Biskaborn, B. K., Vyse, S. A., Courtin, J., Böhmer, T., et al. (2021). Late Pleistocene to Holocene vegetation and climate changes in northwestern Chukotka (Far East Russia) deduced from lakes Ilirney and Rauchaugytyn pollen records. *Boreas* 50, 652–670. doi:10.1111/bor.12521
- Andreev, A. A., Schirrmeister, L., Tarasov, P. E., Ganopolski, A., Brovkin, V., Siebert, C., et al. (2011). Vegetation and climate history in the laptev sea region (arctic Siberia) during late quaternary inferred from pollen records. *Quat. Sci. Rev.* 30, 2182–2199. doi:10.1016/j.quascirev.2010.12.026
- Andreev, A. A., Tarasov, P. E., Schwamborn, G., Ilyashuk, B., Ilyashuk, E., Bobrov, A., et al. (2004). Holocene paleoenvironmental records from nikolay lake, Lena River delta, arctic Russia. *Palaeogeogr. Palaeoclimatol. Palaeoecol.* 209, 197–217. doi:10.1016/j.palaeo.2004.02.010
- Andreev, A. A., Tarasov, P. E., Wennrich, V., Raschke, E., Herzschuh, U., Nowaczyk, N. R., et al. (2014). Late Pliocene and Early Pleistocene vegetation history of northeastern Russian Arctic inferred from the Lake El'gygytyn pollen record. *Clim. Past* 10, 1017–1039. doi:10.5194/cp-10-1017-2014
- Ashastina, K., Kuzmina, S., Rudaya, N., Troeva, E., Schoch, W. H., Römermann, C., et al. (2018). Woodlands and steppes: Pleistocene vegetation in Yakutia's most continental part recorded in the Batagay permafrost sequence. *Quat. Sci. Rev.* 196, 38–61. doi:10.1016/j.quascirev.2018.07.032
- Axmanová, I., Robovský, J., Tichý, L., Danihelka, J., Troeva, E., Protodopov, A., et al. (2020). Habitats of Pleistocene megaherbivores reconstructed from the frozen fauna remains. *Ecography* 43, 703–713. doi:10.1111/ecog.04940
- Baisheva, I., Biskaborn, B. K., Stoof-Leichsenring, K. R., Andreev, A. A., Meucci, S., Lu, Y., et al. (2024). *Biogeochemical and palynological data from Lake Khamra*. PANGAEA. doi:10.1594/PANGAEA.963238
- Baisheva, I., Pestryakova, L., Levina, S., Glücker, R., Biskaborn, B. K., Vyse, S. A., et al. (2023). Permafrost-thaw lake development in Central Yakutia: sedimentary ancient

subsampling. We thank technicians and student workers for the help in laboratory work: Justin Lindemann and Angelique Opitz (TOC and TN); Iris Eder and Janine Klimke (*seada* DNA plants preparation); Holly Blevins and Christina Alt (*seada* DNA diatoms preparation); Lennart Grimm (pollen preparation). We appreciate the help of Thomas Böhmer with creating an overview map. We are grateful to Cathy Jenks for English proofreading. Finally, we express gratitude to Daniel Nývlt for handling our manuscript and to the reviewers Rienk H. Smittenberg and Matěj Roman for their valuable comments on improving this paper.

Conflict of interest

The authors declare that the research was conducted in the absence of any commercial or financial relationships that could be construed as a potential conflict of interest.

Publisher's note

All claims expressed in this article are solely those of the authors and do not necessarily represent those of their affiliated organizations, or those of the publisher, the editors and the reviewers. Any product that may be evaluated in this article, or claim that may be made by its manufacturer, is not guaranteed or endorsed by the publisher.

Supplementary material

The Supplementary Material for this article can be found online at: <https://www.frontiersin.org/articles/10.3389/feart.2024.1354284/full#supplementary-material>

- DNA and element analyses from a Holocene sediment record. *J. Paleolimnol.* 70, 95–112. doi:10.1007/s10933-023-00285-w
- Battarbee, R. W., Jones, V. J., Flower, R. J., Cameron, N. G., Bennion, H., Carvalho, L., et al. (2001). “Diatoms” in tracking environmental change using lake sediments, vol. 3: terrestrial, algal,” in *Siliceous indicators developments in paleoenvironmental research*. Editors J. P. Smol, H. J. B. Birks, and W. M. Last (Dordrecht: Springer Netherlands), 155–202. doi:10.1007/0-306-47668-1_8
- Baumer, M. M., Wagner, B., Meyer, H., Leicher, N., Lenz, M., Fedorov, G., et al. (2021). Climatic and environmental changes in the Yana Highlands of north-eastern Siberia over the last c. 57 000 years, derived from a sediment core from Lake Emanda. *Boreas* 50, 114–133. doi:10.1111/bor.12476
- Bennett, K. D., and Willis, K. J. (2001). “Pollen” in tracking environmental change using lake sediments, vol. 3: terrestrial, algal,” in *Siliceous indicators developments in paleoenvironmental research*. Editors J. P. Smol, H. J. B. Birks, and W. M. Last (Dordrecht: Springer Netherlands), 5–32. doi:10.1007/0-306-47668-1_2
- Berglund, B. E., and Ralska-Jasiewiczowa, M. (1986). *Handbook of Holocene palaeoecology and palaeohydrology*. United States: Wiley.
- Bezrukova, E. V., Tarasov, P. E., Solovieva, N., Krivonogov, S. K., and Riedel, F. (2010). Last glacial–interglacial vegetation and environmental dynamics in southern Siberia: chronology, forcing and feedbacks. *Palaeogeogr. Palaeoclimatol. Palaeoecol.* 296, 185–198. doi:10.1016/j.palaeo.2010.07.020
- Binney, H., Edwards, M. E., Macias-Fauria, M., Lozhkin, A., Anderson, P., Kaplan, J. O., et al. (2017). Vegetation of Eurasia from the last glacial maximum to present: key biogeographic patterns. *Quat. Sci. Rev.* 157, 80–97. doi:10.1016/j.quascirev.2016.11.022
- Biskaborn, B. K., Bolshiyarov, D. Yu., Grigoriev, M. N., Morgenstern, A., Pestryakova, L. A., Tsubizov, L. V., et al. (2021a). *Russian-German Cooperation: expeditions to Siberia in 2020*. Alfred-Wegener-Institut, Helmholtz-Zentrum für Polar-und Meeresforschung. United States: EPIC. doi:10.48433/BZPM_0756_2021
- Biskaborn, B. K., Herzschuh, U., Bolshiyarov, D., Savelieva, L., and Diekmann, B. (2012). Environmental variability in northeastern Siberia during the last ~13,300 yr inferred from lake diatoms and sediment–geochemical parameters. *Palaeogeogr. Palaeoclimatol. Palaeoecol.* 329–330, 22–36. doi:10.1016/j.palaeo.2012.02.003
- Biskaborn, B. K., Herzschuh, U., Bolshiyarov, D., Savelieva, L., Zibulski, R., and Diekmann, B. (2013a). Late Holocene thermokarst variability inferred from diatoms in a lake sediment record from the Lena Delta, Siberian Arctic. *J. Paleolimnol.* 49, 155–170. doi:10.1007/s10933-012-9650-1
- Biskaborn, B. K., Herzschuh, U., Bolshiyarov, D. Y., Schwamborn, G., and Diekmann, B. (2013b). Thermokarst processes and depositional events in a tundra lake, northeastern Siberia: thermokarst processes in a siberian tundra lake. *Permafrost. Periglac. Process.* 24, 160–174. doi:10.1002/ppp.1769
- Biskaborn, B. K., Nazarova, L., Kröger, T., Pestryakova, L. A., Syrykh, L., Pfalz, G., et al. (2021b). Late Quaternary climate reconstruction and lead-lag relationships of biotic and sediment–geochemical indicators at Lake Bolshoe Toko, Siberia. *Front. Earth Sci.* 9, 737353. doi:10.3389/feart.2021.737353
- Biskaborn, B. K., Nazarova, L., Pestryakova, L. A., Syrykh, L., Funck, K., Meyer, H., et al. (2019). Spatial distribution of environmental indicators in surface sediments of Lake Bolshoe Toko, Yakutia, Russia. *Biogeosciences* 16, 4023–4049. doi:10.5194/bg-16-4023-2019
- Biskaborn, B. K., Subetto, D. A., Savelieva, L. A., Vakhrameeva, P. S., Hansche, A., Herzschuh, U., et al. (2016). Late Quaternary vegetation and lake system dynamics in north-eastern Siberia: implications for seasonal climate variability. *Quat. Sci. Rev.* 147, 406–421. doi:10.1016/j.quascirev.2015.08.014
- Bjune, A. E., Greve Alsos, I., Brendryen, J., Edwards, M. E., Hafliadason, H., Johansen, M. S., et al. (2022). Rapid climate changes during the Lateglacial and the early Holocene as seen from plant community dynamics in the Polar Urals, Russia. *J. Quat. Sci.* 37, 805–817. doi:10.1002/jqs.3352
- Blaauw, M., and Christen, J. A. (2011). Flexible paleoclimate age–depth models using an autoregressive gamma process. *Bayesian Anal.* 6. doi:10.1214/11-BA618
- Bobrov, A. E., Kupriyanova, L. A., Litvintseva, M. V., and Tarasevich, V. F. (1983). *Spores and pollen of gymnosperms from the flora of the European part of the USSR*. Leningrad: Nauka, 206. (in Russian).
- Boeskorov, G. G. (2004). The North of eastern Siberia: refuge of mammoth fauna in the Holocene. *Gondwana Res.* 7, 451–455. doi:10.1016/S1342-937X(05)70796-6
- Boyer, F., Mercier, C., Bonin, A., Le Bras, Y., Taberlet, P., and Coissac, E. (2016). obitools: a unix-inspired software package for DNA metabarcoding. *Mol. Ecol. Resour.* 16, 176–182. doi:10.1111/1755-0998.12428
- Brodie, J. F., Roland, C. A., Stehn, S. E., and Smirnova, E. (2019). Variability in the expansion of trees and shrubs in boreal Alaska. *Ecology* 100, e02660. doi:10.1002/ecy.2660
- Brubaker, L. B., Anderson, P. M., Edwards, M. E., and Lozhkin, A. V. (2005). Beringia as a glacial refugium for boreal trees and shrubs: new perspectives from mapped pollen data. *J. Biogeogr.* 32, 833–848. doi:10.1111/j.1365-2699.2004.01203.x
- Cao, X., Tian, F., Li, F., Gaillard, M.-J., Rudaya, N., Xu, Q., et al. (2019). Pollen-based quantitative land-cover reconstruction for northern Asia covering the last 40 ka cal BP. *Clim. Past* 15, 1503–1536. doi:10.5194/cp-15-1503-2019
- Capo, E., Giguet-Covex, C., Rouillard, A., Nota, K., Heintzman, P. D., Vuillemin, A., et al. (2021). Lake sedimentary DNA research on past terrestrial and aquatic biodiversity: overview and recommendations. *Quaternary* 4, 6. doi:10.3390/quat4010006
- Chelnokova, S. M., Chikina, I. D., and Radchenko, S. A. (1988). *Geologic map of Yakutia P-48,49, 1 : 1 000 000*. Leningrad: VSEGEI.
- Clarke, C. L., Edwards, M. E., Gielly, L., Ehrlich, D., Hughes, P. D. M., Morozova, L. M., et al. (2019). Persistence of arctic-alpine flora during 24,000 years of environmental change in the Polar Urals. *Sci. Rep.* 9, 19613. doi:10.1038/s41598-019-55989-9
- Courtin, J., Andreev, A. A., Raschke, E., Bala, S., Biskaborn, B. K., Liu, S., et al. (2021). Vegetation changes in southeastern Siberia during the late Pleistocene and the Holocene. *Front. Ecol. Evol.* 9, 625096. doi:10.3389/fevo.2021.625096
- Courtin, J., Perfumo, A., Andreev, A. A., Opel, T., Stoof-Leichsenring, K. R., Edwards, M. E., et al. (2022). Pleistocene glacial and interglacial ecosystems inferred from ancient DNA analyses of permafrost sediments from Batagay megaslump, East Siberia. *Environ. DNA* edn3, 1265–1283. doi:10.1002/edn3.336
- Courtin, J., Stoof-Leichsenring, K. R., Lisovski, S., Alsos, I. G., Biskaborn, B. K., Diekmann, B., et al. (2024). Potential plant extinctions with the loss of the Pleistocene mammoth-steppe. *Nat. Commun. in revision*.
- Crate, S., Ulrich, M., Habeck, J. O., Desyatkin, A. R., Desyatkin, R. V., Fedorov, A. N., et al. (2017). Permafrost livelihoods: A transdisciplinary review and analysis of thermokarst-based systems of indigenous land use. *Anthropocene* 18, 89–104. doi:10.1016/j.ancene.2017.06.001
- Crump, S. E., Miller, G. H., Power, M., Sepúlveda, J., Dildar, N., Coghlan, M., et al. (2019). Arctic shrub colonization lagged peak postglacial warmth: molecular evidence in lake sediment from Arctic Canada. *Glob. Change Biol.* 25, 4244–4256. doi:10.1111/gcb.14836
- Dallmeyer, A., Kleinen, T., Claussen, M., Weitzel, N., Cao, X., and Herzschuh, U. (2022). The deglacial forest conundrum. *Nat. Commun.* 13, 6035. doi:10.1038/s41467-022-33646-6
- Del Val, C., Barea, J. M., and Azcón-Aguilar, C. (1999). Diversity of arbuscular mycorrhizal fungus populations in heavy-metal-contaminated soils. *Appl. Environ. Microbiol.* 65, 718–723. doi:10.1128/aem.65.2.718-723.1999
- Demske, D., Heumann, G., Granoszewski, W., Nita, M., Mamakowa, K., Tarasov, P. E., et al. (2005). Late glacial and Holocene vegetation and regional climate variability evidenced in high-resolution pollen records from Lake Baikal. *Glob. Planet. Change* 46, 255–279. doi:10.1016/j.gloplacha.2004.09.020
- Diekmann, B., Pestryakova, L., Nazarova, L., Subetto, D., Tarasov, P. E., Stauch, G., et al. (2016). Late Quaternary lake dynamics in the Verkhoyansk Mountains of Eastern Siberia: implications for climate and glaciation history. *Polarforschung* 86, 97–110. doi:10.2312/POLARFORSCHUNG.86.2.97
- Doughty, C. E., Wolf, A., and Field, C. B. (2010). Biophysical feedbacks between the Pleistocene megafauna extinction and climate: the first human-induced global warming? *Geophys. Res. Lett.* 37, L15703. doi:10.1029/2010GL043985
- Dulias, K., Stoof-Leichsenring, K. R., Pestryakova, L. A., and Herzschuh, U. (2017). Sedimentary DNA versus morphology in the analysis of diatom–environment relationships. *J. Paleolimnol.* 57, 51–66. doi:10.1007/s10933-016-9926-y
- Edwards, M. E., Anderson, P. M., Brubaker, L. B., Ager, T. A., Andreev, A. A., Bigelow, N. H., et al. (2000). Pollen-based biomes for Beringia 18,000, 6000 and 0 14C yr BP. *J. Biogeogr.* 27, 521–554. doi:10.1046/j.1365-2699.2000.00426.x
- Epp, L. S., Zimmermann, H. H., and Stoof-Leichsenring, K. R. (2019). “Sampling and extraction of ancient DNA from sediments,” in *Ancient DNA: methods and protocols methods in molecular biology*. Editors B. Shapiro, A. Barlow, P. D. Heintzman, M. Hofreiter, J. L. A. Pajjmans, and A. E. R. Soares (New York, NY: Springer), 31–44. doi:10.1007/978-1-4939-9176-1_5
- ESA Land Cover CCI project team and Defourny, P. (2019). ESA Land Cover Climate Change Initiative (Land_Cover_cci): Global Land Cover Maps, Version 2.0.7. Centre for Environmental Data Analysis. Available at: <https://catalogue.ceda.ac.uk/uuid/b382eb6679d44b8b0e68ea4ef4b701c> (Accessed July 20, 2023).
- Evans, K. M., Wortley, A. H., and Mann, D. G. (2007). An assessment of potential diatom “barcode” genes (cox1, rbcL, 18S and ITS rDNA) and their effectiveness in determining relationships in Sellaphora (Bacillariophyta). *Protist* 158, 349–364. doi:10.1016/j.protis.2007.04.001
- Fedorov, A., Vasilyev, N., Torgovkin, Y., Shestakova, A., Varlamov, S., Zheleznyak, M., et al. (2018). Permafrost-landscape map of the republic of Sakha (Yakutia) on a scale 1:1,500,000. *Geosciences* 8, 465. doi:10.3390/geosciences8120465
- Firsova, A. D., Chebykin, E. P., Kopyrina, L. I., Rodionova, E. V., Chensky, D. A., Gubin, N. A., et al. (2021). Post-glacial diatom and geochemical records of ecological status and water level changes of Lake Vorota, Western Beringia. *J. Paleolimnol.* 66, 407–437. doi:10.1007/s10933-021-00214-9
- GBIF (2023). GBIF. Available at: <https://www.gbif.org/> (Accessed October 27, 2023).
- Geng, R., Andreev, A. A., Kruse, S., Heim, B., van Geffen, F., Pestryakova, L., et al. (2022). Modern pollen assemblages from lake sediments and soil in East Siberia and relative pollen productivity estimates for major taxa. *Front. Ecol. Evol.* 10, 837857. doi:10.3389/fevo.2022.837857

- Giguët-Coxev, C., Ficetola, G. F., Walsh, K., Poulenard, J., Bajard, M., Fouinat, L., et al. (2019). New insights on lake sediment DNA from the catchment: importance of taphonomic and analytical issues on the record quality. *Sci. Rep.* 9, 14676. doi:10.1038/s41598-019-50339-1
- Glückler, R., Geng, R., Grimm, L., Baisheva, I., Herzsuh, U., Stooß-Leichsenring, K. R., et al. (2022). Holocene wildfire and vegetation dynamics in Central Yakutia, Siberia, reconstructed from lake-sediment proxies. *Front. Ecol. Evol.* 10. doi:10.3389/fevo.2022.962906
- Glückler, R., Herzsuh, U., Kruse, S., Andreev, A., Vyse, S. A., Winkler, B., et al. (2021). Wildfire history of the boreal forest of south-western Yakutia (Siberia) over the last two millennia documented by a lake-sediment charcoal record. *Biogeosciences* 18, 4185–4209. doi:10.5194/bg-18-4185-2021
- Guy-Ohlson, D. (1992). Botryococcus as an aid in the interpretation of palaeoenvironment and depositional processes. *Rev. Palaeobot. Palynology* 71, 1–15. doi:10.1016/0034-6667(92)90155-A
- Hagedorn, F., Shiyatov, S. G., Mazepa, V. S., Devi, N. M., Grigor'ev, A. A., Bartysh, A. A., et al. (2014). Treeline advances along the Urals mountain range - driven by improved winter conditions? *Glob. Change Biol.* 20, 3530–3543. doi:10.1111/gcb.12613
- Heinecke, L., Epp, L. S., Reschke, M., Stooß-Leichsenring, K. R., Mischke, S., Plessen, B., et al. (2017). Aquatic macrophyte dynamics in Lake Karakul (Eastern Pamir) over the last 29 cal ka revealed by sedimentary ancient DNA and geochemical analyses of macrofossil remains. *J. Paleolimnol.* 58, 403–417. doi:10.1007/s10933-017-9986-7
- Hendy, C. H., and Hall, B. L. (2006). The radiocarbon reservoir effect in proglacial lakes: examples from Antarctica. *Earth Planet. Sci. Lett.* 241, 413–421. doi:10.1016/j.epsl.2005.11.045
- Herzsuh, U. (2020). Legacy of the Last Glacial on the present-day distribution of deciduous versus evergreen boreal forests. *Glob. Ecol. Biogeogr.* 29, 198–206. doi:10.1111/gcb.13018
- Herzsuh, U., Birks, H. J. B., Laepple, T., Andreev, A. A., Melles, M., and Brigham-Grette, J. (2016). Glacial legacies on interglacial vegetation at the Pliocene-Pleistocene transition in NE Asia. *Nat. Commun.* 7, 11967. doi:10.1038/ncomms11967
- Herzsuh, U., Böhmer, T., Chevalier, M., Hébert, R., Dallmeyer, A., Li, C., et al. (2023). Regional pollen-based Holocene temperature and precipitation patterns depart from the Northern Hemisphere mean trends. *Clim. Past* 19, 1481–1506. doi:10.5194/cp-19-1481-2023
- Herzsuh, U., Li, C., Böhmer, T., Postl, A. K., Heim, B., Andreev, A. A., et al. (2022). LegacyPollen 1.0: a taxonomically harmonized global late Quaternary pollen dataset of 2831 records with standardized chronologies. *Earth Syst. Sci. Data* 14, 3213–3227. doi:10.5194/essd-14-3213-2022
- Herzsuh, U., Mischke, S., Meyer, H., Plessen, B., and Zhang, C. (2010). Lake nutrient variability inferred from elemental (C, N, S) and isotopic ($\delta^{13}C$, $\delta^{15}N$) analyses of aquatic plant macrofossils. *Quat. Sci. Rev.* 29, 2161–2172. doi:10.1016/j.quascirev.2010.05.011
- Herzsuh, U., Pestryakova, L. A., Savelieva, L. A., Heinecke, L., Böhmer, T., Biskaborn, B. K., et al. (2013). Siberian larch forests and the ion content of thaw lakes form a geochemically functional entity. *Nat. Commun.* 4, 2408. doi:10.1038/ncomms3408
- Herzsuh, U., Zhang, C., Mischke, S., Herzsuh, R., Mohammadi, F., Mingram, B., et al. (2005). A late Quaternary lake record from the Qilian Mountains (NW China): evolution of the primary production and the water depth reconstructed from macrofossil, pollen, biomarker, and isotope data. *Glob. Planet. Change* 46, 361–379. doi:10.1016/j.gloplacha.2004.09.024
- Huang, S., Herzsuh, U., Pestryakova, L. A., Zimmermann, H. H., Davydova, P., Biskaborn, B. K., et al. (2020). Genetic and morphologic determination of diatom community composition in surface sediments from glacial and thermokarst lakes in the Siberian Arctic. *J. Paleolimnol.* 64, 225–242. doi:10.1007/s10933-020-00133-1
- Huang, S., Stooß-Leichsenring, K. R., Liu, S., Courtin, J., Andreev, A. A., Pestryakova, L. A., et al. (2021). Plant sedimentary ancient DNA from Far East Russia covering the last 28,000 years reveals different assembly rules in cold and warm climates. *Front. Ecol. Evol.* 9, 15. doi:10.3389/fevo.2021.763747
- Hudson, S. M., Waddington, C., Pears, B., Ellis, N., Parker, L., Hamilton, D., et al. (2023). Lateglacial and early Holocene palaeoenvironmental change and human activity at killerby quarry, north yorkshire, UK. *J. Quat. Sci.* 38, 403–422. doi:10.1002/jqs.3488
- Hughes-Allen, L., Bouchard, F., Hatté, C., Meyer, H., Pestryakova, L. A., Diekmann, B., et al. (2021). 14,000-year carbon accumulation dynamics in a Siberian lake reveal catchment and lake productivity changes. *Front. Earth Sci.* 9, 710257. doi:10.3389/feart.2021.710257
- IPCC (2022). *Climate change 2022 – impacts, adaptation and vulnerability: working group II contribution to the sixth assessment report of the intergovernmental panel on climate change*. 1st ed. Cambridge: Cambridge University Press. doi:10.1017/9781009325844
- Isaev, A. P., Protopopov, A. V., Protopopova, V. V., Egorova, A. A., Timofeyev, P. A., Nikolaev, A. N., et al. (2010). "Vegetation of Yakutia: elements of ecology and plant sociology," in *The far north plant and vegetation*. Editors E. I. Troeva, A. P. Isaev, M. M. Cherosov, and N. S. Karpov (Dordrecht: Springer Netherlands), 143–260. doi:10.1007/978-90-481-3774-9_3
- Jørgensen, T., Haile, J., Möller, P., Andreev, A., Boessenkool, S., Rasmussen, M., et al. (2012). A comparative study of ancient sedimentary DNA, pollen and macrofossils from permafrost sediments of northern Siberia reveals long-term vegetational stability. *Mol. Ecol.* 21, 1989–2003. doi:10.1111/j.1365-294X.2011.05287.x
- Juggins, S. (2022). Rioja: analysis of quaternary science data. Available at: <https://cran.r-project.org/web/packages/rioja/index.html> (Accessed October 12, 2023).
- Kanz, C., Aldebert, P., Althorpe, N., Baker, W., Baldwin, A., Bates, K., et al. (2005). The EMBL Nucleotide sequence database. *Nucleic Acids Res.* 33, D29–D33. doi:10.1093/nar/gki098
- Karachurina, S., Rudaya, N., Frolova, L., Kuzmina, O., Cao, X., Chepinoga, V., et al. (2023). Terrestrial vegetation and lake aquatic community diversity under climate change during the mid-late Holocene in the Altai Mountains. *Palaeogeogr. Palaeoclimatol. Palaeoecol.* 623, 111623. doi:10.1016/j.palaeo.2023.111623
- Katamura, F., Fukuda, M., Bosikov, N. P., and Desyatkin, R. V. (2009). Charcoal records from thermokarst deposits in central Yakutia, eastern Siberia: implications for forest fire history and thermokarst development. *Quat. Res.* 71, 36–40. doi:10.1016/j.yqres.2008.08.003
- Katamura, F., Fukuda, M., Bosikov, N. P., Desyatkin, R. V., Nakamura, T., and Moriizumi, J. (2006). Thermokarst Formation and vegetation dynamics inferred from a palynological study in central Yakutia, eastern Siberia, Russia. *Arct. Antarct. Alp. Res.* 38, 561–570. doi:10.1657/1523-0430(2006)38[561:TFAVDI]2.0.CO;2
- Kaufman, D., McKay, N., Routson, C., Erb, M., Dätwyler, C., Sommer, P. S., et al. (2020). Holocene global mean surface temperature, a multi-method reconstruction approach. *Sci. Data* 7, 201. doi:10.1038/s41597-020-0530-7
- Kienast, F., Schirmer, L., Siebert, C., and Tarasov, P. (2005). Palaeobotanical evidence for warm summers in the East Siberian Arctic during the last cold stage. *Quat. Res.* 63, 283–300. doi:10.1016/j.yqres.2005.01.003
- Kleinen, T., Gromov, S., Steil, B., and Brovkin, V. (2023). Atmospheric methane since the Last Glacial Maximum was driven by wetland sources. *Clim. Past* 19 (5), 1081–1099. doi:10.5194/cp-19-1081-2023
- Klemm, J., Herzsuh, U., and Pestryakova, L. A. (2016). Vegetation, climate and lake changes over the last 7000 years at the boreal treeline in north-central Siberia. *Quat. Sci. Rev.* 147, 422–434. doi:10.1016/j.quascirev.2015.08.015
- Kobe, F., Bezrukova, E. V., Leipe, C., Shchetnikov, A. A., Goslar, T., Wagner, M., et al. (2020). Holocene vegetation and climate history in Baikal Siberia reconstructed from pollen records and its implications for archaeology. *Archaeol. Res. Asia* 23, 100209. doi:10.1016/j.ara.2020.100209
- Kobe, F., Hoelzmann, P., Gliwa, J., Olschewski, P., Peskov, S. A., Shchetnikov, A. A., et al. (2022a). Lateglacial–Holocene environments and human occupation in the Upper Lena region of Eastern Siberia derived from sedimentary and zooarchaeological data from Lake Ochaul. *Quat. Int.* 623, 139–158. doi:10.1016/j.quaint.2021.09.019
- Kobe, F., Leipe, C., Shchetnikov, A. A., Hoelzmann, P., Gliwa, J., Olschewski, P., et al. (2022b). Not herbs and forbs alone: pollen-based evidence for the presence of boreal trees and shrubs in Cis-Baikal (Eastern Siberia) derived from the Last Glacial Maximum sediment of Lake Ochaul. *J. Quat. Sci.* 37, 868–883. doi:10.1002/jqs.3290
- Kostrova, S. S., Biskaborn, B. K., Pestryakova, L. A., Fernandoy, F., Lenz, M. M., and Meyer, H. (2021). Climate and environmental changes of the Lateglacial transition and Holocene in northeastern Siberia: evidence from diatom oxygen isotopes and assemblage composition at Lake Emanda. *Quat. Sci. Rev.* 259, 106905. doi:10.1016/j.quascirev.2021.106905
- Kruse, S. (2021). R_Rarefaction 1.0. Available at: https://github.com/StefanKruse/R_Rarefaction (Accessed October 28, 2023).
- Kruse, S., and Herzsuh, U. (2022). Regional opportunities for tundra conservation in the next 1000 years. *eLife* 11, e75163. doi:10.7554/eLife.75163
- Kupriyanova, L. A., and Alyoshina, L. A. (1972). *Pollen and spores of plants from the flora of European part of USSR*. Leningrad: Academy of Sciences USSR, Komarov Botanical Institute, 171. (in Russian).
- Kupriyanova, L. A., and Alyoshina, L. A. (1978). *Pollen and spores of plants from the flora of European part of USSR*. Leningrad: Academy of Sciences USSR, Komarov Botanical Institute, 183. (in Russian).
- Li, F., Li, W., Li, F., Long, Y., Guo, S., Li, X., et al. (2022). Global projections of future wilderness decline under multiple IPCC Special Report on Emissions Scenarios. *Resour. Conserv. Recycl.* 177, 105983. doi:10.1016/j.resconrec.2021.105983
- Li, K., Stooß-Leichsenring, K. R., Liu, S., Jia, W., Liao, M., Liu, X., et al. (2021). Plant sedimentary DNA as a proxy for vegetation reconstruction in eastern and northern Asia. *Ecol. Indic.* 132, 108303. doi:10.1016/j.ecolind.2021.108303
- Liu, S., Stooß-Leichsenring, K. R., Kruse, S., Pestryakova, L. A., and Herzsuh, U. (2020). Holocene vegetation and plant diversity changes in the North-Eastern Siberian treeline region from pollen and sedimentary ancient DNA. *Front. Ecol. Evol.* 8, 560243. doi:10.3389/fevo.2020.560243
- Lougheed, V., Crosbie, B., and Chow-Fraser, P. (2001). Primary determinants of macrophyte community structure in 62 marshes across the Great Lakes basin: latitude, land use, and water quality effects. *Can. J. Fish. Aquatic Sci.* 58, 1603–1612. doi:10.1139/cjfas-58-8-1603

- Lozhkin, A. V., Anderson, P. M., Matrosova, T. V., Minyuk, P. S., Brigham-Grette, J., and Melles, M. (2007). Continuous record of environmental changes in Chukotka during the last 350 thousand years. *Russ. J. Pac. Geol.* 1, 550–555. doi:10.1134/S1819714007060048
- Mackay, A. W. (2007). The paleoclimatology of Lake Baikal: a diatom synthesis and prospectus. *Earth-Science Rev.* 82, 181–215. doi:10.1016/j.earscirev.2007.03.002
- Margold, M., Jansen, J. D., Gurinov, A. L., Codilean, A. T., Fink, D., Preusser, F., et al. (2016). Extensive glaciation in transbaikalia, Siberia, at the last glacial maximum. *Quat. Sci. Rev.* 132, 161–174. doi:10.1016/j.quascirev.2015.11.018
- Mariash, H. L., Cazzanelli, M., Rautio, M., Hamerlik, L., Wooller, M. J., and Christoffersen, K. S. (2018). Changes in food web dynamics of low Arctic ponds with varying content of dissolved organic carbon. *Arct. Antarct. Alp. Res.* 50, S100016. doi:10.1080/15230430.2017.1414472
- Matveev, I. A. (1989). *Agricultural Atlas of the republic Sakha (Yakutia)* (Moscow: Nauka), 115. (in Russian).
- Meyers, P. A., and Teranes, J. L. (2002). “Sediment organic matter” in tracking environmental change using lake sediments, vol. 2,” in *Physical and geochemical methods*. Editors W. M. Last, and J. P. Smol (Dordrecht: Kluwer Academic Publishers), 239–269. doi:10.1007/0-306-47670-3_9
- Miesner, T., Herzschuh, U., Pestryakova, L. A., Wiczorek, M., Zakharov, E. S., Kolmogorov, A. I., et al. (2022). Forest structure and individual tree inventories of northeastern Siberia along climatic gradients. *Earth Syst. Sci. Data* 14, 5695–5716. doi:10.5194/essd-14-5695-2022
- Monteath, A. J., Gaglioti, B. V., Edwards, M. E., and Froese, D. (2021). Late Pleistocene shrub expansion preceded megafauna turnover and extinctions in eastern Beringia. *Proc. Natl. Acad. Sci.* 118, e2107977118. doi:10.1073/pnas.2107977118
- Müller, S., Tarasov, P. E., Andreev, A. A., Tütken, T., Gartz, S., and Diekmann, B. (2010). Late Quaternary vegetation and environments in the Verkhoyansk Mountains region (NE Asia) reconstructed from a 50-kyr fossil pollen record from Lake Billyakh. *Quat. Sci. Rev.* 29, 2071–2086. doi:10.1016/j.quascirev.2010.04.024
- Nazarova, L., Lüpfer, H., Subetto, D., Pestryakova, L., and Diekmann, B. (2013). Holocene climate conditions in central Yakutia (Eastern Siberia) inferred from sediment composition and fossil chironomids of Lake Temje. *Quat. Int.* 290–291, 264–274. doi:10.1016/j.quaint.2012.11.006
- Niemeyer, B., Epp, L. S., Stoof-Leichsenring, K. R., Pestryakova, L. A., and Herzschuh, U. (2017). A comparison of sedimentary DNA and pollen from lake sediments in recording vegetation composition at the Siberian treeline. *Mol. Ecol. Resour.* 17, e46–e62. doi:10.1111/1755-0998.12689
- Niemeyer, B., Klemm, J., Pestryakova, L. A., and Herzschuh, U. (2015). Relative pollen productivity estimates for common taxa of the northern Siberian Arctic. *Rev. Palaeobot. Palynology* 221, 71–82. doi:10.1016/j.revpalbo.2015.06.008
- Obu, J., Westermann, S., Bartsch, A., Berdnikov, N., Christiansen, H. H., Dashtseren, A., et al. (2019). Northern Hemisphere permafrost map based on TTOP modelling for 2000–2016 at 1 km² scale. *Earth-Science Rev.* 193, 299–316. doi:10.1016/j.earscirev.2019.04.023
- Odland, A. (1992). A synecological investigation of *Matteuccia struthiopteris*-dominated stands in Western Norway. *Vegetatio* 102, 69–95. doi:10.1007/BF00031704
- Oksanen, J., Simpson, G. L., Blanchet, F. G., Kindt, R., Legendre, P., Minchin, P. R., et al. (2022). *Vegan: community ecology package*. Available at: <https://cran.r-project.org/web/packages/vegan/index.html> (Accessed October 12, 2023).
- Parducci, L., Bennett, K. D., Ficetola, G. F., Alsos, I. G., Suyama, Y., Wood, J. R., et al. (2017). Ancient plant DNA in lake sediments. *New Phytol.* 214, 924–942. doi:10.1111/nph.14470
- Pearson, R. G., Phillips, S. J., Lorant, M. M., Beck, P. S. A., Damoulas, T., Knight, S. J., et al. (2013). Shifts in Arctic vegetation and associated feedbacks under climate change. *Nat. Clim. Change* 3, 673–677. doi:10.1038/nclimate1858
- Pelánková, B., Kuneš, P., Chytrý, M., Jankovská, V., Ermakov, N., and Svobodová-Svitavská, H. (2008). The relationships of modern pollen spectra to vegetation and climate along a steppe–forest–tundra transition in southern Siberia, explored by decision trees. *Holocene* 18, 1259–1271. doi:10.1177/0959683608096600
- Pestryakova, L. A., Herzschuh, U., Gorodnichev, R., and Wetterich, S. (2018). The sensitivity of diatom taxa from Yakutian lakes (north-eastern Siberia) to electrical conductivity and other environmental variables. *Polar Res.* 37, 1485625. doi:10.1080/17518369.2018.1485625
- Pestryakova, L. A., Herzschuh, U., Wetterich, S., and Ulrich, M. (2012). Present-day variability and Holocene dynamics of permafrost-affected lakes in central Yakutia (Eastern Siberia) inferred from diatom records. *Quat. Sci. Rev.* 51, 56–70. doi:10.1016/j.quascirev.2012.06.020
- Philippson, B. (2013). The freshwater reservoir effect in radiocarbon dating. *Herit. Sci.* 1, 24. doi:10.1186/2050-7445-1-24
- Plants of the World Online (2023). Kew science. Available at: <https://powo.science.kew.org/> (Accessed December 11, 2023).
- Plasteeva, N. A., Gasilin, V. V., Devjashin, M. M., and Kosintsev, P. A. (2020). Holocene distribution and extinction of ungulates in northern Eurasia. *Biol. Bull. Russ. Acad. Sci.* 47, 981–995. doi:10.1134/S1062359020080105
- Pratap, S., and Markonis, Y. (2022). The response of the hydrological cycle to temperature changes in recent and distant climatic history. *Prog. Earth Planet. Sci.* 9, 30. doi:10.1186/s40645-022-00489-0
- R Core Team (2023). *R: a language and environment for statistical computing*. Vienna, Austria: R Foundation for Statistical Computing.
- Reille, M. (1992). *Pollen et spores d'Europe et d'Afrique du nord*. Marseille: Laboratoire de Botanique Historique et Palynologie, 327.
- Reille, M. (1995). *Pollen et spores d'Europe et d'Afrique du nord Supplement 1*. Marseille: Laboratoire de Botanique Historique et Palynologie, 191.
- Reille, M. (1998). *Pollen et spores d'Europe et d'Afrique du nord Supplement 2*. Marseille: Laboratoire de Botanique Historique et Palynologie, 530.
- Reimer, P. J., Austin, W. E. N., Bard, E., Bayliss, A., Blackwell, P. G., Bronk Ramsey, C., et al. (2020). The IntCal20 northern Hemisphere radiocarbon age calibration curve (0–55 cal kBP). *Radiocarbon* 62, 725–757. doi:10.1017/RDC.2020.41
- Revéret, A., Rijal, D. P., Heintzman, P. D., Brown, A. G., Stoof-Leichsenring, K. R., and Alsos, I. G. (2023). Environmental DNA of aquatic macrophytes: the potential for reconstructing past and present vegetation and environments. *Freshw. Biol.* 68, 1929–1950. doi:10.1111/fwb.14158
- Rosenbaum, J. G., Reynolds, R. L., Adam, D. P., Drexler, J., Sarna-Wojcicki, A. M., and Whitney, G. C. (1996). Record of middle Pleistocene climate change from Buck Lake, Cascade Range, southern Oregon—Evidence from sediment magnetism, trace-element geochemistry, and pollen. *Geol. Soc. Am. Bull.* 108, 1328–1341. doi:10.1130/0016-7606(1996)108<1328:ROMPCC>2.3.CO;2
- Schulte, L., Li, C., Lisovski, S., and Herzschuh, U. (2022a). Forest-permafrost feedbacks and glacial refugia help explain the unequal distribution of larch across continents. *J. Biogeogr.* 49, 1825–1838. doi:10.1111/jbi.14456
- Schulte, L., Meucci, S., Stoof-Leichsenring, K. R., Heikam, T., Schmidt, N., von Hippel, B., et al. (2022b). *Larix* species range dynamics in Siberia since the Last Glacial captured from sedimentary ancient DNA. *Commun. Biol.* 5, 570. doi:10.1038/s42003-022-03455-0
- Shahgedanova, M. (2002). “Climate at present and in the historical past,” in *The physical geography of northern Eurasia*. Editor M. Shahgedanova (Oxford: Oxford University Press), 3, 70–102.
- Shestakova, A. A., Fedorov, A. N., Torgovkin, Y. I., Konstantinov, P. Y., Vasylyev, N. F., Kalinicheva, S. V., et al. (2021). Mapping the main characteristics of permafrost on the basis of a permafrost-landscape map of Yakutia using GIS. *Land* 10, 462. doi:10.3390/land10050462
- Soininen, E. M., Gauthier, G., Bilodeau, F., Berteaux, D., Gielly, L., Taberlet, P., et al. (2015). Highly overlapping winter diet in two sympatric Lemming species revealed by DNA metabarcoding. *PLoS ONE* 10, e0115335. doi:10.1371/journal.pone.0115335
- Sonstebo, J. H., Gielly, L., Brysting, A. K., Elven, R., Edwards, M., Haile, J., et al. (2010). Using next-generation sequencing for molecular reconstruction of past Arctic vegetation and climate. *Mol. Ecol. Resour.* 10, 1009–1018. doi:10.1111/j.1755-0998.2010.02855.x
- Stenina, A. S. (2009). Diatom algae (Bacillariophyta) in the lakes of the eastern Bolshezemelskaya tundra. *Saktyykar. Biol. Inst. Komi Sci. Cent. Russ. Acad. Sci.*, 176.
- Stieg, A., Biskaborn, B. K., Herzschuh, U., Strauss, J., Pestryakova, L., and Meyer, H. (2023). Hydroclimate extreme events detected by a sub-decadal diatom oxygen isotope record of the last 220 years from Lake Khamra, Siberia. *Clim. Past Discuss.*, 1–42. doi:10.5194/cp-2023-85
- Stockmarr, J. (1971). Tablets with spores used in absolute pollen analysis. *Pollen Spores* 13, 615–621.
- Stoof-Leichsenring, K. R., Bernhardt, N., Pestryakova, L. A., Epp, L. S., Herzschuh, U., and Tiedemann, R. (2014). A combined paleolimnological/genetic analysis of diatoms reveals divergent evolutionary lineages of *Stauriosira* and *Stauriosirella* (Bacillariophyta) in Siberian lake sediments along a latitudinal transect. *J. Paleolimnol.* 52, 77–93. doi:10.1007/s10933-014-9779-1
- Stoof-Leichsenring, K. R., Dulias, K., Biskaborn, B. K., Pestryakova, L. A., and Herzschuh, U. (2020). Lake-depth related pattern of genetic and morphological diatom diversity in boreal Lake Bolshoe Toko, Eastern Siberia. *PLoS ONE* 15, e0230284. doi:10.1371/journal.pone.0230284
- Stoof-Leichsenring, K. R., Epp, L. S., Trauth, M. H., and Tiedemann, R. (2012). Hidden diversity in diatoms of Kenyan Lake Naivasha: a genetic approach detects temporal variation. *Mol. Ecol.* 21, 1918–1930. doi:10.1111/j.1365-294X.2011.05412.x
- Stoof-Leichsenring, K. R., Herzschuh, U., Pestryakova, L. A., Klemm, J., Epp, L. S., and Tiedemann, R. (2015). Genetic data from algae sedimentary DNA reflect the influence of environment over geography. *Sci. Rep.* 5, 12924. doi:10.1038/srep12924
- Stoof-Leichsenring, K. R., Huang, S., Liu, S., Jia, W., Li, K., Liu, X., et al. (2022). Sedimentary DNA identifies modern and past macrophyte diversity and its environmental drivers in high-latitude and high-elevation lakes in Siberia and China. *Limnol. Oceanogr.* 67, 1126–1141. doi:10.1002/lno.12061

- Stuart, A. J. (1999). "Late Pleistocene megafaunal extinctions," in *Extinctions in near time*. Editor R. D. E. MacPhee (Boston: Springer), 257–269. doi:10.1007/978-1-4757-5202-1_11
- Stuenzi, S. M., Boike, J., Gädeke, A., Herzsich, U., Kruse, S., Pestryakova, L. A., et al. (2021). Sensitivity of ecosystem-protected permafrost under changing boreal forest structures. *Environ. Res. Lett.* 16, 084045. doi:10.1088/1748-9326/ac153d
- Subetto, D. A., Nazarova, L. B., Pestryakova, L. A., Syrykh, L. S., Andronikov, A. V., Biskaborn, B., et al. (2017). Paleolimnological studies in Russian northern Eurasia: a review. *Contemp. Problems Ecol.* 10, 327–335. doi:10.1134/S1995425517040102
- Taberlet, P., Coissac, E., Pompanon, F., Gielly, L., Miquel, C., Valentini, A., et al. (2007). Power and limitations of the chloroplast trnL (UAA) intron for plant DNA barcoding. *Nucleic Acids Res.* 35, e14. doi:10.1093/nar/gkl938
- Tarasov, P. E., Bezrukova, E. V., and Krivonogov, S. K. (2009). Late Glacial and Holocene changes in vegetation cover and climate in southern Siberia derived from a 15 kyr long pollen record from Lake Kotokel. *Clim. Past* 5, 285–295. doi:10.5194/cp-5-285-2009
- Tarasov, P. E., Leipe, C., and Wagner, M. (2021). Environments during the spread of anatomically modern humans across Northern Asia 50–10 cal kyr BP: what do we know and what would we like to know? *Quat. Int.* 596, 155–170. doi:10.1016/j.quaint.2020.10.030
- Tarasov, P. E., Webb III, T., Andreev, A. A., Afanas'eva, N. B., Berezina, N. A., Bezusko, L. G., et al. (1998). Present-day and mid-Holocene biomes reconstructed from pollen and plant macrofossil data from the former Soviet Union and Mongolia. *J. Biogeogr.* 25, 1029–1053. doi:10.1046/j.1365-2699.1998.00236.x
- Tchebakova, N. M., Parfenova, E., and Soja, A. J. (2009). The effects of climate, permafrost and fire on vegetation change in Siberia in a changing climate. *Environ. Res. Lett.* 4, 045013. doi:10.1088/1748-9326/4/4/045013
- Tian, F., Cao, X., Dallmeyer, A., Lohmann, G., Zhang, X., Ni, J., et al. (2018). Biome changes and their inferred climatic drivers in northern and eastern continental Asia at selected times since 40 cal ka BP. *Veg. Hist. Archaeobotany* 27, 365–379. doi:10.1007/s00334-017-0653-8
- Troeva, E. I., Isaev, A. P., Cherosov, M. M., and Karpov, N. S. (2010). *The far north: plant biodiversity and ecology of Yakutia*. Dordrecht: Springer. doi:10.1007/978-90-481-3774-9
- Ulrich, M., Wetterich, S., Rudaya, N., Frolova, L., Schmidt, J., Siegert, C., et al. (2017). Rapid thermokarst evolution during the mid-Holocene in Central Yakutia, Russia. *Holocene* 27, 1899–1913. doi:10.1177/0959683617708454
- van den Boogaart, K. G., Tolosana-Delgado, R., and Bren, M. (2023). Compositions: compositional data analysis. R package version 2.0-6.
- van Geel, B. (2001). "Non-Pollen palynomorphs" in tracking environmental change using lake sediments, vol. 3: terrestrial, algal," in *Siliceous indicators developments in paleoenvironmental research*. Editors J. P. Smol, H. J. B. Birks, and W. M. Last (Dordrecht: Springer Netherlands), 99–119. doi:10.1007/0-306-47668-1_6
- von Hippel, B., Stoof-Leichsenring, K. R., Schulte, L., Seeber, P., Epp, L. S., Biskaborn, B. K., et al. (2022). Long-term fungus–plant covariation from multi-site sedimentary ancient DNA metabarcoding. *Quat. Sci. Rev.* 295, 107758. doi:10.1016/j.quascirev.2022.107758
- Vyse, S. A., Herzsich, U., Andreev, A. A., Pestryakova, L. A., Diekmann, B., Armitage, S. J., et al. (2020). Geochemical and sedimentological responses of arctic glacial Lake Ilirney, Chukotka (far east Russia) to palaeoenvironmental change since ~51.8 ka BP. *Quat. Sci. Rev.* 247, 106607. doi:10.1016/j.quascirev.2020.106607
- Vyse, S. A., Herzsich, U., Pfalz, G., Pestryakova, L. A., Diekmann, B., Nowaczyk, N., et al. (2021). Sediment and carbon accumulation in a glacial lake in Chukotka (Arctic Siberia) during the Late Pleistocene and Holocene: combining hydroacoustic profiling and down-core analyses. *Biogeosciences* 18, 4791–4816. doi:10.5194/bg-18-4791-2021
- Wang, D., Wang, C., Yang, X., and Lu, J. (2005). Winter northern Hemisphere surface air temperature variability associated with the arctic oscillation and north atlantic oscillation. *Geophys. Res. Lett.* 32. doi:10.1029/2005GL022952
- Werner, K., Tarasov, P. E., Andreev, A. A., Müller, S., Kienast, F., Zech, M., et al. (2010). A 12.5-kyr history of vegetation dynamics and mire development with evidence of Younger Dryas larch presence in the Verkhoyansk Mountains, East Siberia, Russia. *Boreas* 39, 56–68. doi:10.1111/j.1502-3885.2009.00116.x
- Wetterich, S., Herzsich, U., Meyer, H., Pestryakova, L., Plessen, B., Lopez, C. M. L., et al. (2008). Evaporation effects as reflected in freshwaters and ostracod calcite from modern environments in Central and Northeast Yakutia (East Siberia, Russia). *Hydrobiologia* 614, 171–195. doi:10.1007/s10750-008-9505-y
- Willerslev, E., Davison, J., Moora, M., Zobel, M., Coissac, E., Edwards, M. E., et al. (2014). Fifty thousand years of Arctic vegetation and megafaunal diet. *Nature* 506, 47–51. doi:10.1038/nature12921
- Woodwell, G. M., and Mackenzie, F. T. (1995). *Biotic feedbacks in the global climatic system: will the warming feed the warming?* Oxford: Oxford University Press.
- Wu, B., and Wang, J. (2002). Winter arctic oscillation, siberian high and east asian winter monsoon. *Geophys. Res. Lett.* 29, 3-1-3–4. doi:10.1029/2002GL015373
- Zimmermann, H. H., Raschke, E., Epp, L. S., Stoof-Leichsenring, K. R., Schirrmeister, L., Schwamborn, G., et al. (2017a). The history of tree and shrub taxa on Bol'shoy Lyakhovskiy Island (New Siberian Archipelago) since the Last Interglacial uncovered by sedimentary ancient DNA and pollen data. *Genes* 8, 273. doi:10.3390/genes8100273
- Zimmermann, H. H., Raschke, E., Epp, L. S., Stoof-Leichsenring, K. R., Schwamborn, G., Schirrmeister, L., et al. (2017b). Sedimentary ancient DNA and pollen reveal the composition of plant organic matter in Late Quaternary permafrost sediments of the Buor Khaya Peninsula (north-eastern Siberia). *Biogeosciences* 14, 575–596. doi:10.5194/bg-14-575-2017